TÉCNICO LISBOA

# Modelling of naphtha cracking for olefins production

**João Miguel Monteiro Marcos**

Thesis to obtain the Master of Science Degree in

**Chemical Engineering**

Supervisors: Prof. Dr. Carla Isabel Costa Pinheiro
Dr. Štěpán Špatenka

## Examination Committee

| | |
|---|---|
| Chairperson: | Prof. Dr. Maria Filipa Gomes Ribeiro |
| Supervisor: | Prof. Dr. Carla Isabel Costa Pinheiro |
| Member of the Committee: | Prof. Dr. José Manuel Félix Madeira Lopes |

**December 2016**

**“No thief, however skillful, can rob one of knowledge, and that is why knowledge is the best and safest treasure to acquire.”**

- L. Frank Baum

# Acknowledgements

First of all, I would like to thank Professor Carla Pinheiro, Professor Henrique Matos, and especially Professor Costas Pantelides for presenting the possibility of taking an internship at Process Systems Enterprise Ltd., a seven-month experience which highly contributed to my professional and personal growth.

I would also like to thank my supervisors, both from PSE and IST. To Štěpán and Sreekumar, thank you for sharing your knowledge and experience during these past seven months, and for always finding the time to answer my questions. To Professor Carla, thank you for always showing availability to help solve various problems and for your guidance and assistance throughout the process of writing this Dissertation.

I would like to acknowledge everyone at PSE for making me feel welcome and creating a good work environment. Special acknowledgment to all the interns with whom I shared this new experience.

To my housemates, thank you for the great times and for making this experience of living abroad something I will never forget.

Finally, I would like to show my deepest gratitude to my family and friends, particularly to my parents and my sister for all the love and support in every moment of my life.

# Resumo

A produção de etileno e propileno a partir de nafta através de craqueamento térmico é um pilar da indústria química. Este processo é conduzido em fornalhas que opera a elevadas temperaturas, sendo que a otimização do seu funcionamento é necessária para manter rentabilidade.

No presente trabalho, foi desenvolvido em gPROMS®, um modelo de uma fornalha de craqueamento de nafta com uma serpentina do tipo SRT-VI. O modelo da fornalha foi usado para validação de mecanismos cinéticos presentes na literatura, usando dados típicos de cracking de nafta como fator comparativo.

Foi desenvolvida uma afinação dos mecanismos cinéticos, ao adicionar componentes, conjuntos de reações, e afinando alguns dos parâmetros cinéticos do esquema reacional, levando a resultados próximos de valores típicos para o cracking de nafta. Os rendimentos previstos apresentam desvios menores que 5% para os produtos principais, olefinas leves (etileno e propileno) e cerca de 15% para aromáticos.

**Palavras-Chave:** modelação, craqueamento térmico, nafta, etano, propano, cinética, fornalha

# Abstract

The production of ethylene and propylene from naphtha via thermal cracking is a cornerstone of the chemical industry. This process is carried out in furnaces operating at high temperature and optimal operation of these furnaces is necessary to maintain profitability.

In the present work, a model of a naphtha cracking furnace with a typical SRT-VI coil was developed in gPROMS®. This furnace model was used to validate implemented kinetics present in literature against typical data for naphtha cracking.

The model predictions are compared to typical naphtha cracking yields to assess the gap. A tuning of the implemented kinetics was carried out, by adding new components, new sets of reactions and tuning a few of the kinetic parameters in the reaction scheme, leading to good predictions of yields for naphtha cracking. The results show yield deviations of less than 5% for the main products, light olefins (ethylene and propylene) and around 15% for aromatics.

**Keywords:** modelling, steam cracking, naphtha, ethane, propane, kinetics, furnace

# Contents

# List of Tables

# List of Figures

# Nomenclature

**Acronyms**

| | |
|---|---|
| AGO | Atmospheric gas oil. |
| BTX | Benzene, toluene and xylenes. |
| CIP | Coil inlet pressure. |
| CIT | Coil inlet temperature. |
| COP | Coil outlet pressure. |
| COT | Coil outlet temperature. |
| EBZ | Ethylbenzene. |
| EO | Ethylene oxide. |
| FCC | Fluid catalytic cracking. |
| FM | Flow Multiplier. |
| GO | Gas oil. |
| HC | Hydrocarbon. |
| HCR | Hydrocracking. |
| HDT | Hydrotreating/hydroprocessing. |
| KAIST | Korea Advanced Institute of Science and Technology. |
| KPIC | Korean Petrochemical Industry Co. |
| LPG | Liquefied petroleum gas. |
| PD | Propadiene. |
| PE | Polyethylene. |
| PFR | Plug flow reactor. |
| PS | Polystyrene. |
| PSSA | Pseudo-steady state assumption. |
| PVC | Polyvinyl chloride. |

| | |
|---|---|
| Q8 | Kuwait Petroleum International. |
| QAPCO | Qatar Petrochemical Company. |
| SRT | Short Residence Time |
| TLE | Transfer-line exchanger. |
| TST | Tube skin temperature. |

**Greek Symbols**

| | |
|---|---|
| $\alpha$ | Angle (°). |
| $\Delta_f H^0$ | Standard-state heat of formation. |
| $\Delta G^0_{form}$ | Standard-state Gibbs free energy of formation. |
| $\Delta P$ | Pressure drop. |
| $\Delta z$ | Infinitesimal length of the control volume ($m$). |
| $\varepsilon$ | Wall roughness ($m$), dispersion energy ($J$) or emissivity. |
| $\lambda$ | Thermal conductivity ($kW\ m^{-1}\ k^{-1}$). |
| $\mu$ | Viscosity ($Pa \cdot s$). |
| $\nu$ | Stoichiometric coefficient. |
| $\rho$ | Process gas density ($kg\ m^{-3}$). |
| $\sigma$ | Stefan-Boltzmann constant ($kW\ m^{-2}\ K^{-4}$). |
| $\theta_R$ | Residence time. |

**Roman symbols**

| | |
|---|---|
| $A$ | Cross-sectional area ($m^2$). |
| C | Molar concentration ($kmol\ mol^{-3}$). |
| $C_P$ | Process gas heat capacity. |
| $f_{bend}$ | Friction factor of bends. |
| $f_{Fanning}$ | Fanning friction factor. |
| $h$ | Specific enthalpy ($kJ\ kg^{-1}$) or heat transfer coefficient ($kW\ m^{-2}\ K^{-1}$). |
| $k$ | Reaction constant ($mol^{n-1}\ m^{-3n+3}\ s^{-1}$). |

| | |
|---|---|
| $k_0$ | Pre-exponential factor ($mol^{n-1}\ m^{-3n+3}\ s^{-1}$). |
| $k_B$ | Boltzmann constant ($m^2\ kg\ s^{-2}\ K^{-1}$). |
| $L$ | Reactor/coil length ($m$). |
| $MW$ | Molecular weight ($kg\ kmol^{-1}$). |
| $N$ | Mass flux ($kg\ m^{-2}\ s^{-1}$) or number (integer). |
| $n$ | Reaction order. |
| nB | Number of bends in the coil. |
| Nu | Nusselt number. |
| $P$ | Pressure. |
| $Pr$ | Prandtl number. |
| q | Heat flux ($kJ\ m^{-2}\ s^{-1}$). |
| R | Radius ($m$) or ideal gas constant ($J\ mol^{-1}\ K^{-1}$). |
| r | Rate of reaction/formation ($mol\ m^{-3}\ s^{-1}$). |
| $Re$ | Reynolds number. |
| $T$ | Temperature ($K$). |
| $T_{flame}$ | Effective flame temperature ($K$). |
| $T_{flue}$ | Absolute flue gas temperature ($K$). |
| TMT | Tube metal temperature ($K$). |
| v | Process gas linear velocity ($m\ s^{-1}$). |
| $Y$ | Product yield. |

**Subscripts**

| | |
|---|---|
| avg | Stands for average. |
| $b$ | Refers to backward reaction constant. |
| bend | Refers to coil bends. |
| coke | Refers to deposited coke. |
| ext | Stands for external. |
| $f$ | Refers to forward reaction constant. |

| | |
|---|---|
| form | Stands for formation. |
| i | Refers to chemical species. |
| int | Stands for internal. |
| *j* | Refers to chemical reactions. |
| process | Refers to the process stream. |

**Superscripts**

| | |
|---|---|
| 0 | Refers to standard-state. |

# Glossary

| | |
|---|---|
| **CFD** | Grouping of species which are generally isomers or homologous species with similar reactivity in order to reduce the total number of species in a kinetic model. |
| **Gas condensates** | A low-density mixture of hydrocarbons that are present as gaseous components in raw natural gas and are extracted therefrom by condensation. |
| **Group additivity method** | A group additivity method is a technique that allows to predict properties from molecular structures. |
| **Incipient cracking temperature** | Temperature just below the cracking reaction temperature, normally achieved at the radiant coil inlet. |
| **Lumping** | Grouping of species which are generally isomers or homologous species with similar reactivity in order to reduce the total number of species in a kinetic model. |
| **PSSA** | Pseudo-steady state assumption that states the time rate of change of the concentration of all species covered by this assumption can be considered as zero. |
| **Pygas** | Pyrolysis gasoline is a $C_5$ to $C_{12}$ product with a high aromatics content produced as a byproduct of high temperature naphtha cracking during ethylene and propylene production. |
| **RKS** | Redlich–Kwong-Soave cubic equation of state is an empirical, algebraic equation that relates temperature, pressure, and volume of gases. |
| **SEMK** | Single-Event Microkinetic Model is a kinetic model consisting of elementary reactions and accounts for all energetically equivalent reaction paths to determine each reaction rate. |
| **SUPERTRAPP** | NIST SUPERTRAPP is a computer database for the prediction of thermodynamic and transport properties of fluid mixtures, based on phase equilibria calculations. |

| | |
|---|---|
| **Straight-run naphtha** | Petroleum cuts composed by C5−C10 hydrocarbons obtained directly from the crude atmospheric distillation unit. |
| **TLE** | Transfer-line exchangers are the exchangers that immediately follow the radiant coil, performing an indirect quenching of the cracked gas to prevent further cracking of valuable reaction products. |

# Chapter 1

# Introduction

Hydrocarbon steam cracking is one of the most important processes in the petrochemical industry, as it is able to produce highly valuable olefins such as ethylene, propylene and butadiene from lower value feedstocks, which usually have fossil fuel origin and range from gaseous feedstocks like ethane and propane, to liquid, heavier feedstocks, such as naphtha, gas oil and gas condensates. From the mentioned feedstocks, naphtha is the most widely used, due to availability, low cost and potential for producing high yields of olefins, namely ethylene and propylene. [1] [2]

Ethylene is the major product of a stream cracking unit, being almost exclusively produced in this process. With a world production of around 1.48 million tonnes/year in 2014 [3], with an annual growth at an average rate of $4\%$, it is the largest volume chemical building block, and it is mainly used for the production of polyethylene, ethylene oxide, vinyl acetate, and ethylbenzene and ethylene dichloride [4], very important components in modern society.

Propylene is considered a co-product of an olefins plant as nearly $60\%$ of its production – 109 million tonnes in 2014 – is associated with ethylene's manufacture. Propylene is a valuable olefin, being responsible for the production of polypropylene, propylene oxide, cumene and isopropanol [5].

The method for the production of olefins from naphtha is through hydrocarbon cracking reactions, which occur in the presence of steam in the radiant coil of the furnace, at temperatures ranging from $700℃$ at the inlet of the coil to $900℃$ at the outlet. The cracking reactions occur via free-radical mechanisms, resulting in (for the cracking of naphtha) yields of ethylene between $25 - 35\%$ and propylene between $14 - 18\%$ [1].

The high temperatures inside the coil favour the formation of coke, which tends to accumulate of the tube walls, leading to reduced heat transfer and increased pressure drops, thus reducing the efficiency of the process and ultimately leading to furnace shutdown.

For a whole-plant optimisation, models capable of predicting the cracking and coking phenomena are essential.

## 1.1 Motivation

The production of ethylene and propylene from naphtha via thermal cracking is a cornerstone of the chemical industry. This process is carried out in furnaces operating at high temperature.

Model based optimisation of these furnaces requires predictive models to represent the cracking and coking phenomena. The current work has the aim of developing such detailed models and in the verification of their predictive capability against typical data for naphtha cracking.

The current work will focus on developing a furnace model, which will be used to implement published kinetic schemes, and to compare simulation results with typical data from naphtha cracking.

## 1.2 State-of-the-art

The steam cracking process is one of the most important in the petrochemical industry, and it has been thoroughly reviewed in engineering encyclopaedias [1] [6], books [7] [8], and several published articles [9] [10].

Several kinetic models describing thermal cracking phenomena are available in published literature, ranging from empirical models [11] [12] to molecular schemes [13-15] and mechanistic/radical ones [16-20].

Finally, several PhD and Master Thesis have focused on the study of the modelling of steam cracking [21-25].

## 1.3 Outline

To begin with, Chapter 2 will focus on reviewing the steam cracking process and the published kinetic mechanisms.

In Chapter 3, an overview of the gPROMS® platform is made, describing the software and reviewing the most relevant tools to be used in the current work.

Chapter 4 describes the mathematical furnace model for naphtha cracking is reviewed, and the main components and functionalities of that model are studied.

Chapter 5 contains the results for the simulation studies performed using the developed model, comparison with typical data and tuning of the kinetic schemes.

Finally, Chapter 6 contains the main conclusions of the current work, discussing what was achieved and proposing possible future work.

# Chapter 2

# Background

In the current section of the work, the main parts of the topic of olefins production from the cracking of naphtha will be reviewed:

First, a brief study of the market of olefins, showing statistics for the current market and predictions for the coming years.

Next, the steam cracking process will be reviewed, with special emphasis on the cracking of naphtha: process description, as well as review of some plants currently operating. The study of the steam cracking process is of most importance in order to be able to develop predictive models for cracking furnaces.

Finally, the cracking reactions will be reviewed, giving a brief overview on the reaction types that occur in the furnace, and by exploring published literature describing the kinetic models made to predict the cracking reactions.

## 2.1 Olefins market

Ethylene and propylene and the main products of any olefin plant, and are highly valued in the petrochemical industry, as they are the building blocks for several types of plastics and pharmaceutical products. Ethylene is almost exclusively produced by the steam cracking process [26], while $60\%$ of propylene is produced by this process.

Ethylene is the major product of a stream cracking unit, with a world production of around 1.48 million tonnes/year in 2014 [3], and an annual growth at an average rate of around $4\%$ for the last five years [1]. It is mainly used for the production of different plastics and pharmaceutical products, such polyethylene, ethylene oxide, vinyl acetate, ethylbenzene and ethylene dichloride [4], being polyethylene the dominant one, due to its importance as a plastic with several applications, accounting for $60\%$ of demand of ethylene.

Propylene production has registered 109 million tonnes in 2014 [1]. It is a valuable olefin, being responsible for the production of polypropylene, propylene oxide, cumene and isopropanol [5].

The market price of these olefins is closely tied to the cost of hydrocarbon feedstock, as this directly affects the cost of production. The table below shows ethylene and propylene prices in Europe as of October 2016 [27].

Table 2.1 - Ethylene and propylene prices in the European market for October 2016.

| **Olefin** | **Price (€/tonne)** |
|---|---|
| Ethylene | 940 |
| Propylene | 725 |

Steam cracking can be designed to use a wide variety of feedstocks, ranging from the gaseous feedstocks, such as ethane, propane and butane, to liquid feedstocks, such as naphtha, gas oils and gas condensates. Ethane and naphtha are the two major feedstock types, in which the plants work at operating rates of $80 - 90\%$ [26]. The current work will focus on the cracking of naphtha.

Naphtha has always dominated the olefins plant feedstock market, especially in the regions of Europe and Asia, due to having competitive prices in comparison with gaseous feedstocks, especially with the recent decrease of crude oil's prices [3], as well as being able to produce many other important secondary products, such as aromatics.

Figure 2.1 compares the various feedstocks used for ethylene production over the years, and makes it evident that naphtha is expected to remain the most prominent feedstock for the production of olefins through steam cracking. [28]

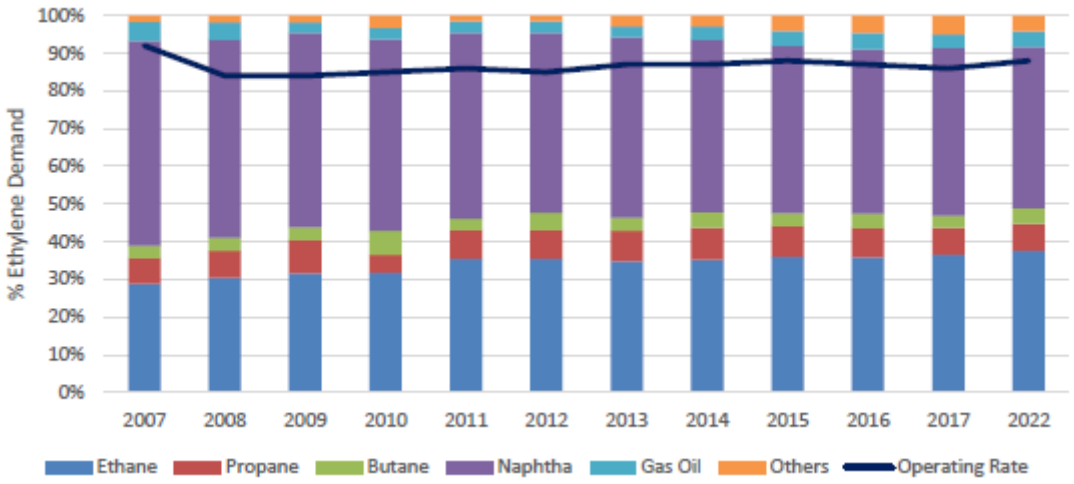


Figure 2.1 - Feedstock comparison for ethylene production.

The capacity for industrial steam cracking units has had a big growth. At the beginning of the industrial ethylene production, in the 1950s, the first plants had capacities of $20 \times 10^3\ t/a$. A decade later, a typical plant capacity had grown to of $60 - 80 \times 10^3\ t/a$. Since then, plant capacity has continued to increase, and currently most of the largest crackers (almost all locates in the Middle East) have ethylene capacities of of $150 \times 10^3\ t/a$, almost 1000 times the capacities of the first plants. [1]

The table below presents a list of modern steam cracker plants, of which some are still projects, starting in the upcoming years. [3]

Table 2.2 - Modern steam cracking projects.

| Company | Location | Capacity ($t/a$) | Start-up |
|---|---|---|---|
| Map Tha Phut Olefins | Thailand | 1.0M | 2010 |
| Indial Oil Corp | India | 850,000 | 2015 |
| Sadara | Saudi Arabia | 1.5M | 2015 |
| Borouge | UAE | 1.5M | 2015 |
| Axiall/Lotte | Louisiana, USA | 1.0M | 2017 |
| Dow Chemical | Texas, USA | 1.5M | 2017 |
| ExxonMobil 1.5m | Texas, USA | 1.5M | 2017 |
| Shell | Pennsylvania, USA | 1.5M | 2018 |

## 2.2 Steam cracking process

Steam cracking of hydrocarbons (pyrolysis reactions) is the main industrial process for the production of olefins, responsible for the production of $98\%$ of the production and $60\%$ of propylene. [1]

A simplified flowsheet of this process is shown in Figure 2.2 [1], detailing the main units of the process as well as the main products. The most important elements of this process are represented by highlighted thicker lines, representing the feed and main products (olefins), as well as the steam cracking furnace, which is the reactor and "heart" of the chemical plant. The operations shown in blue are only present on plants running with liquid feedstocks (such as naphtha).

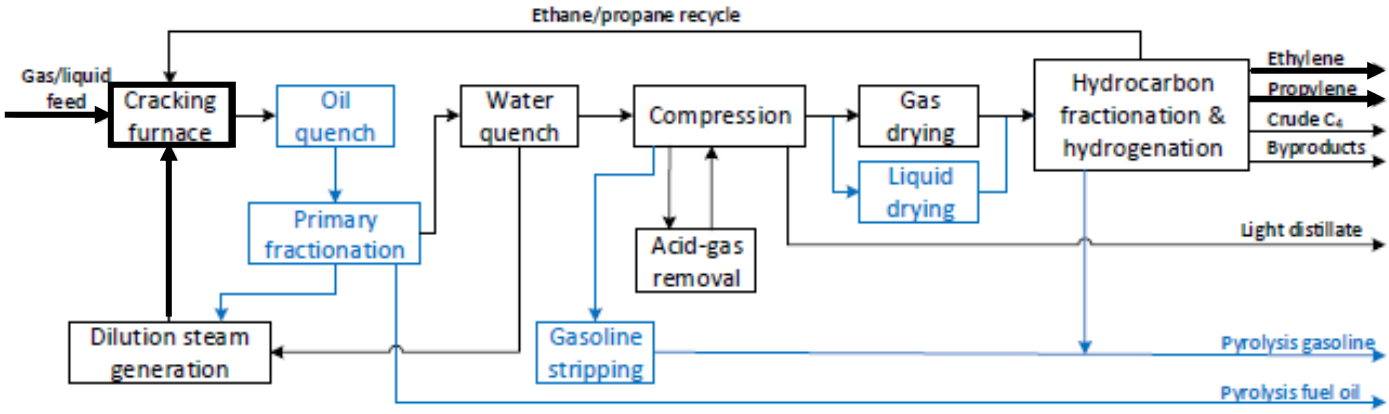


Figure 2.2 - Simplified flowsheet of the steam cracking process.

The cracking furnace (Figures 2.3 and 2.4) is the most important unit of this process, and will be thoroughly reviewed, followed by a brief overview of the other units of the steam cracking process.

The hydrocarbon feedstock enters the furnace in the convection section, where it is pre-heated by heat exchange against flue gases. It is then mixed with steam (dilution steam), and the resulting mixture is further heated to temperatures of $500 - 680$ ℃, which favour the cracking reactions.

This mixture of feed and steam, in the gaseous state, enters the radiant section of the furnace, where radiant coils act as tubular reactors, submitting the hydrocarbons to cracking reactions for periods of $0.1 - 0.5\ s$. This section of the furnace operates at temperatures between $600 - 860$ ℃, which are maintained through heat transfer with a firebox, where fuel burners reach temperatures between $1000 - 1200$ ℃. Due to the endothermicity of the cracking reactions occurring, high heat fluxes are required [1]. For the cracking of naphtha, and depending on the operating conditions (which heavily influence the severity of cracking), the product stream is made up of (in $wt.\%$) $25 - 35$ % of ethylene, $14 - 18$ % of propylene, $4 - 6$ % of butadiene as well as $\sim 14$ % of methane and $5 - 10$ % of aromatics, namely BTX.

After exiting the furnace, the resulting stream, in the gaseous phase, and with a high content on light olefins is subjected to a series of treatments to remove condensates, water and other undesired components before the fractionation step.

The cracked gas then leaves the radiant coil at $800 - 860$ ℃ (coil outlet temperature), and is cooled during a period of $0.02 - 0.1\ s$ to $550 - 650$ ℃ to prevent further cracking of valuable reaction products as well the formation of coke, which tends to occur at higher temperatures. This cooling process occurs in the transfer-line exchangers (TLE), by indirect quenching.

An oil quench, which is only used only for liquid feedstocks, due to higher temperatures at the exit of the radiant coil, is used to reduce the temperature down to around $230$ ℃. [1]

Next, a primary fractionator (gasoline fractionator) is used in order to separate the pyrolysis fuel oil (heavier hydrocarbons) from the main stream. Part of the pyrolysis fuel oil is cooled and recycled back to perform cracked gas quenching.

To be further processed, the hydrocarbon product stream is then cooled to near ambient temperature by means of water quench tower, in which it contacts with a large descending water stream.

To compress the cracked gas, a series of 4 to 6 compression stages with inter-stage coolers is used, allowing the cracked gas to reach pressures up to $35$ bars, while maintaining temperatures below $100$ ℃ [26]. The condensates, as well as water and other heavier components are removed during this cooling process, alongside with $H_2S$ and $CO_2$, which are removed by contacting with an alkaline solution (acid gas removal). [1]

The resulting gas needs to be dried in order to remove water (up to $< 1\ ppm$), in order to proceed for the fractionation equipment. The gas drying is achieved with molecular sieves beds.

Finally, the cracked and now purified gas is chilled and separated into its product streams (ethylene, propylene, crude $C_4$ and pyrolysis gasoline and gas oil), by means of a fractionation train composed by the following distillation columns: demethaniser, deethaniser, depropaniser, debutaniser, ethylene fractionator and propylene fractionator. In order to further increase light olefins yield,

hydrogenation reactions occur, in which acetylene, methylacetylene and propadiene are converted to ethylene and propylene in catalytic hydrogenation beds. [1] [26]

After summarising the main units of a steam cracking plant, a more detailed description of cracking furnace follows, detailing the various phenomena that occur and studying the optimal operating conditions.

## 2.2.1 Cracking Furnace

The cracking furnace is the “heart” of any steam cracking plant, being responsible for the cracking of lower-value feedstocks into higher-value products, such as olefins. The optimal operation of these units is a key factor in maintaining safety, efficiency and profitability of olefin plants.

Figure 2.3 - Furnace section of a naphtha cracking plant.

Cracking furnaces are divided into two main sections: convection section and radiant section (or firebox), as shown in the Figure 2.4 [9] that will be further reviewed in the next section of work.

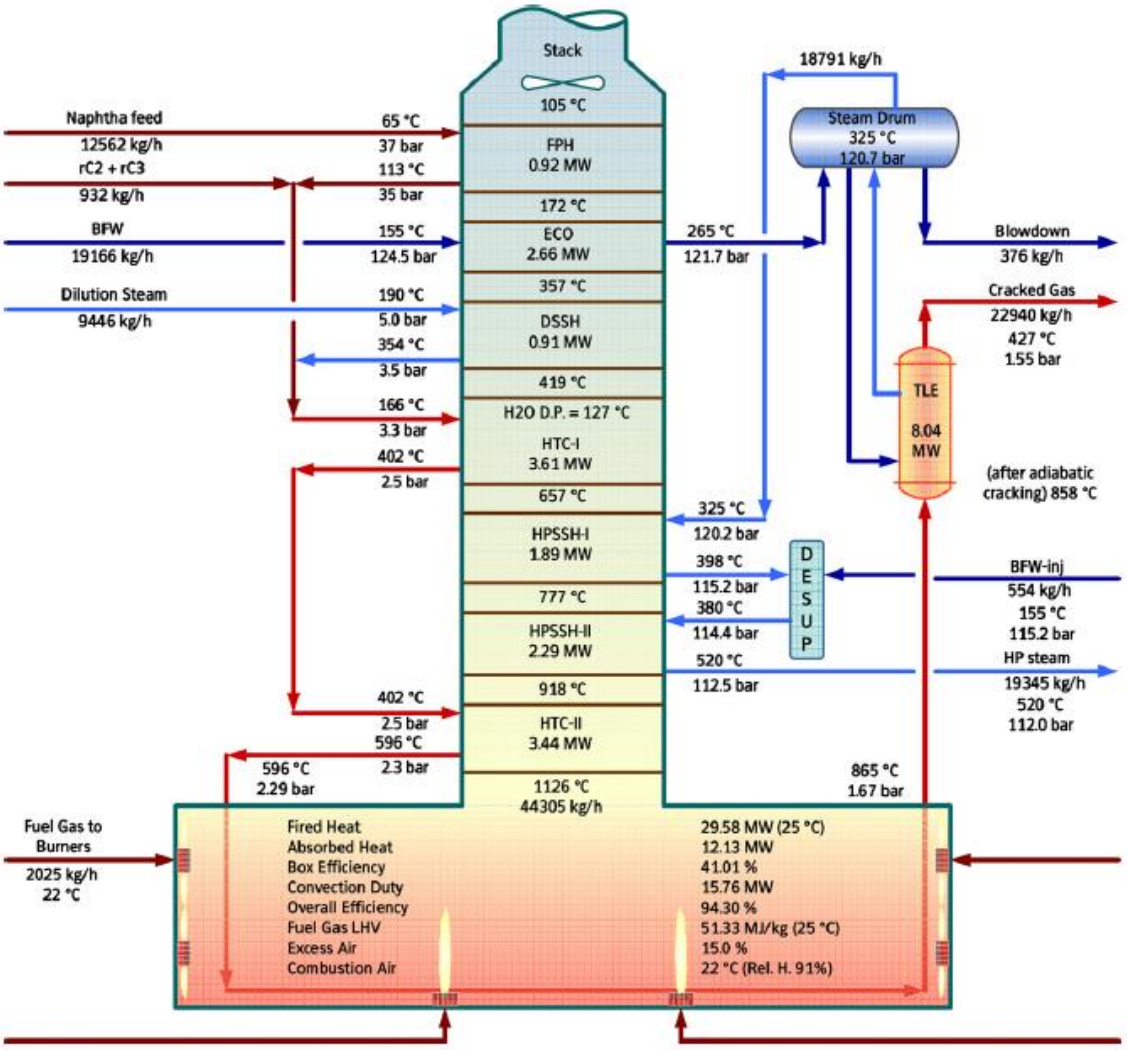


Figure 2.4 - Diagram of a cracking furnace.

### 2.2.1.1 Convection section

This section of the furnace is responsible for pre-heating of the hydrocarbon feed, by convective heat transfer with hot flue gases coming from the radiant section. This allows for energy integration, which is essential for optimisation of any plant.

In section also occurs the mixing with a dilution steam, which is used mainly in order to reduce the hydrocarbon partial pressure inside the coils, which could otherwise lead to high coke formation rates inside the coil. The dilution steam is added to create Steam:Oil ratios ($kg_{steam}/kg_{hydrocarbon}$) of $0.25 - 0.40$ for gaseous feed and $0.40 - 0.55$ in the case of naphtha.

### 2.2.1.2 Radiant section

This section of the furnace is responsible for the cracking of the hydrocarbon feed, which occurs inside the radiant or cracking coils, at high temperatures (up to $860$ ℃ in the case of naphtha cracking) and low pressure ($1.50 - 2.75$ bar) [1].

The preheated gases from the convection section (at temperatures of $500 - 600$ ℃) are fed into this radiant section, where they are heated to cracking-favouring temperatures, by heat transfer with the firebox burners, that reach temperatures as high as $1000 - 1200$ ℃. The burners can be mounted on the wall and/or floor, thus influencing the firing type and the heat transfer between the firebox and the radiant coils. Due to the fact that the cracking reactions are highly endothermic, high heat fluxes ($75 - 85\ kW/m^2$of coil) are needed, in order to keep the radiant coil at high temperatures that favour the pyrolysis.

Nearly $90\%$ of the heat transfer in this section is accomplished by radiation mechanisms, namely between hot flue gases/coil and between refractory walls/coil [26].

Cracking coils can have several different configurations (as seen in the figure below), ranging from single tubes to branching parallel tubes of different diameters, depending on the furnace design and on the feedstock. Typical coil dimensions are usually $40 - 90\ m$ in length, diameters from $3 - 20\ cm$.

Figure 2.5 - Industrial cracking coil.

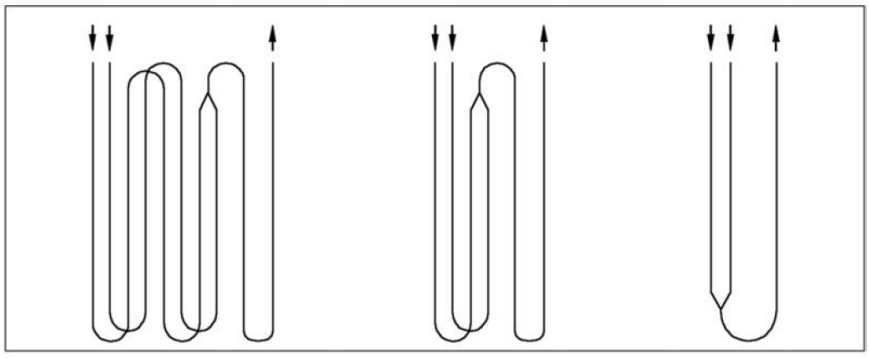

Figure 2.6 - Schematic of different coil configurations.

## 2.3 Steam cracking reactions

Cracking refers to a reaction in which a large hydrocarbon produces a higher number of smaller molecules. This type of reaction can occur through two mechanisms: thermal cracking, in which the breakdown of the hydrocarbon molecule is induced by higher temperatures, and catalytic cracking, in which a selective catalyst promotes the breakage of the bonds in the hydrocarbon molecule.

Both are of extreme importance in the petrochemical industry, but in the case of steam cracking, it is exclusively based on thermal cracking, which occurs in the presence of steam.

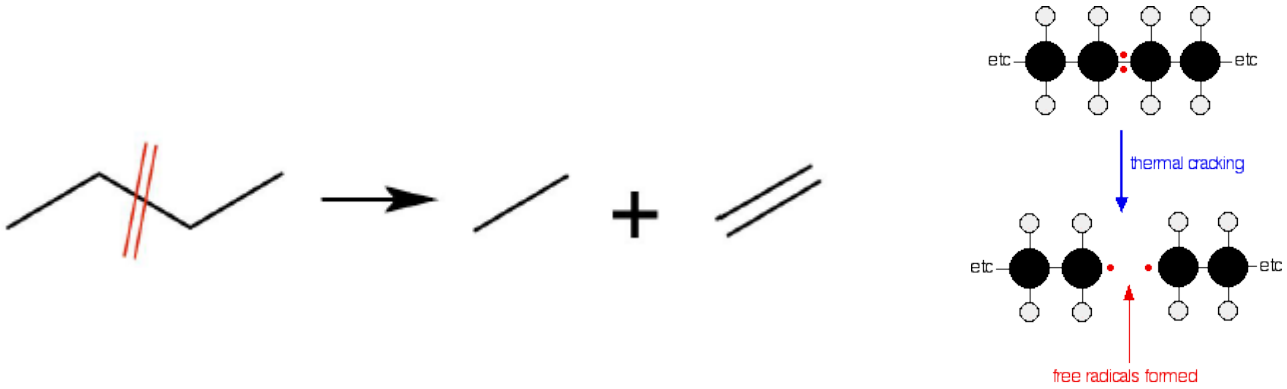


Figure 2.7 - Cracking reactions.

### 2.3.1 Thermodynamics

A thermodynamic analysis determines whether or not a specific reaction path is favourable. At relatively low temperatures, unsaturated hydrocarbons are more unstable than the saturated compounds from which they were formed. At high temperatures, however, the opposite is observed [29]. This observation leads to two major conclusions: it explains why the steam cracking at operated at such high temperatures ($700 - 900$ ℃), and also explains the high reactivity of olefins at relatively low temperatures, making them highly flexible components for organic synthesis.

Cracking reactions lead to an increase of the number of molecules, which explains the fact that in order to promote the cracking reactions, pressures must be kept as low as possible ($1.5 - 2.75$ bar).

Given the fact that the $C - C$ bond ($345\ kJ/mol$) is weaker than the $C - H$ ($413\ kJ/mol$) [30], thermal activation causes the scission of the $C - C$ bond easier, thus cracking the molecule, as opposed to the $C - H$ bond, whose breakage causes the production of olefins by dehydrogenation.

## 2.3.2 Kinetic mechanisms

It is widely accepted that the largest part of gas phase hydrocarbon pyrolysis occurs through a free radical mechanism, characterized by a vast number of species and reactions.

The kinetic mechanism is summarised by the following reaction classes [16] [31].

**1) Initiation and termination reactions**

These reactions involve either the C-C bond scission, thus forming two smaller radicals (Eq. 2.1a), or the formation of a new bond (C-C or C-H) as two radicals come together and produce a single molecule (Eq. 2.1b).

$$R_1 + R_2 \rightarrow R_1^* + R_2^* \quad (2.1a)$$

$$R_1^* + R_2^* \rightarrow R_1 + R_2 \quad (2.1b)$$

**2) Propagation reactions**

After the initiation step, radical species undergo a series of propagation reactions in which a radical reacts with a molecule and produces a smaller molecule and a new radical, keeping the reaction chain going. These reactions can be of different types:

A. Hydrogen abstraction

Smaller reactive radicals, such as hydrogen, methyl, ethyl, propyl and vinyl radicals abstract a hydrogen atom from another molecule, creating both a new molecule and a new radicals. Kinetic parameters of these reactions are mainly function of the H abstracting radical and the site from which H-atom is abstracted.

$$R_1 + R_2^* \rightarrow R_1^* + R_2 \quad (2.2)$$

B. Radical addition

Radicals react with olefins, thus forming less saturated compounds and a new radical. Addition reactions explain the presence in cracked gases of heavier products than those initially present in the feed.

$$R_1^* + R_2 = R_3 \rightarrow R_1 - R_2 - R_3^* \quad (2.3)$$

C. Radical isomerisation

Responsible for the transfer of the active radical position within the molecule. This can be accomplished whether by intramolecular H-abstractions or by an internal addition of the radical position on unsaturated bonds. Internal radical addition on double bonds, typical for olefin and aromatic radicals, favours the formation of five or six membered cyclic components, precursors of aromatic compounds.

$$R_1^* - R_2 - R_3 - R_4 \leftrightarrow R_1 - R_2 - R_3^* - R_4 \tag{2.4}$$

**3) Condensation reactions**

Smaller molecules (ethylene and propylene) and radicals (vinyl, benzyl), when in abundance, experience successive addition and condensation reactions, leading to heavier components.

$$R_1 = R_2 + R_3 = R_4 \rightarrow R_3 - R_4 - R_3 = R_4 \tag{2.5}$$

## 2.3.3 Kinetic models

Steam pyrolysis of hydrocarbons has a great deal of importance for the petrochemical industry, so the need arises to develop kinetic models capable of predicting the product distribution in a cracking process, for different feedstocks and varying operating conditions.

Three major types of kinetic models have been developed:

**1. Empirical or regression models**

Empirical are the simplest models, based on historical or calculated data sets and, being mainly used by operators. These are appropriate process computer control and optimisation in plants, as they require little computing power. This type of models, based on regression, rarely give accurate results when falling out of the range of the empirical data field and lack for being feedstock-specific, thus being inappropriate when it comes to simulate the furnace behaviour with different operating conditions and several feedstocks. For this reason, this type of models will not be considered for the current work.

## 2. Molecular models

Molecular models reflect a more advanced approach to hydrocarbon pyrolysis, applying global molecular reactions and describing the main products as a function of the feedstock.

Even though these models have been published and implemented, they are only able to provide reasonable results to simple cases of hydrocarbon thermal cracking, namely lighter feedstocks, such as ethane and propane. When it comes to naphtha, the more complex nature of the reactions occurring make it so the predictions of the product distribution are rather unsatisfactory.

Still, it is worth to further review these models, as they might prove useful for the prediction of simple cracking cases, or to extract reactions and add them to complement more complex models.

Several literature has been published on this topic, and the main ones will now be reviewed.

Sundaram and Froment [14] published a very simple set of molecular reaction models and their kinetic parameters for the cracking of ethane, propane and their mixtures. This model contained about 10 reactions.

The same authors same authors later reported the same kind of kinetic models, for the cracking of i-butane, n-butane and for ethane/propane/n-butane mixtures, now with more reactions per model (rounding 11-23), being the able to cover practically all the gaseous feedstocks for steam cracking [32].

These same authors later reported a mechanistic model [18], which will be discussed in the next segment of the work.

Kumar and Kunzru [15] proposed a set of 22 molecular reactions for naphtha pyrolysis. The authors represented naphtha as a pseudo-pure compound, and its decomposition was defined by a single reaction with the initial selectivity determined experimentally, thus giving the model a rather empirical nature as well.

Belohlav et al. [13] proposed a set of 64 molecular reactions involving several species up to $C_5$ for a wide range of feedstocks, mainly focusing on naphtha. This scheme was meant to be used in conjunction with another mechanistic scheme, which was not disclosed, making it unlikely to use the published scheme to accurately predict plant data. The same authors later published a semi-mechanistic scheme, used for more specific feedstocks [33].

Table 2.3 - Molecular kinetic models found in literature.

| Kinetic model | Feedstock | No. of species | No. of reactions |
|---|---|---|---|
| Sundaram and Froment **[14]** | Gaseous (up to $C_4$) | 11 | 23 |
| Kumar and Kunzru **[15]** | Naphtha | 15 | 22 |
| Belohlav **[13]** | Ethane, LPG and Naphtha | 55 | 64 |

### 3. Mechanistic (free-radical) models

These models are based on schemes of free-radicals, are much more complex, being able to cover a wide variety of feedstocks and operating conditions, and can be easily extrapolated. For these reasons, these models are the only models capable of accurately simulating thermal cracking phenomena and predict product yields, proving themselves as particularly appropriate for the design, operation and optimisation of modern olefins plants.

In terms of kinetic models, these will be the main focus of the current work, and the main available schemes will now be reviewed.

Barazandeh et al. [34] published a rather simple model for naphtha cracking which encompasses elements empirical, molecular and mechanistic approaches. This model comprises a set of 22 molecular reactions, 8 radical reactions, 7 coke formation reactions and one single empirical equation for the naphtha cracking itself, yielding smaller products which then react according to the other reactions.

After their work on the molecular models and realising its limitations, Sundaram and Froment, reported [18] a kinetic scheme consisting of 133 reactions and including 42 chemical species with number of carbon atoms up to $C_4$. This model greatly improved on its predecessor, being able to much better predict data for gaseous feedstock.

Joo and Park, from KAIST, South Korea, developed a PC-based software, CRACKER, which includes a reaction scheme for naphtha cracking comprising a total of 231 reactions between 79 chemical species up to $C_9$ [20] [22]. The published scheme can be found in Appendix B.

Towfighi et al. [19] [35] from Olefin Research Group of Tarbiat Modares University, Iran, developed a simulation software for the prediction of product yields and run lengths of ethane and naphtha cracking furnaces. The detailed mechanistic kinetic scheme is said to involve 1230 reactions and 122 molecular and radical species, but the available data references account for only 150 reactions, involving 54 components, used for the cracking of naphtha.

Keyvanloo et al. [36] presented a scheme of 96 reactions including components up to $C_6$. This work heavily focused on the lumping of components, which removed complexity.

Table 2.4 - Radical kinetic models found in literature.

| Kinetic model | Feedstock | No. of species | No. of reactions |
|---|---|---|---|
| Sundaram and Froment **[18]** | Up to $C_5$ | 38 | 133 |
| Joo **[20] [22]** | Naphtha (up to $C_9$) | 86 | 230 |
| Towfighi **[19] [35]** | Naphtha (up to $C_8$) | 54 | 150 |
| Keyvanloo **[36]** | Naphtha (up to $C_6$) | 45 | 96 |

Apart of kinetic models involving reaction schemes published in literature, some other mechanistic model software has been developed, with the objective of more accurately predict the pyrolysis data. The four most prominent softwares are: SPYRO® [37], CRACKSIM, CRACKER [20] and SHAHAB [38].

SPYRO® is Technip's proprietary yield prediction software for the steam cracking process, having been established for over 30 years allowing for feedstock selection, optimal ethylene furnace operation, being one of the key instruments for design, operation and optimisation of cracking coils [37]. It currently comprises over $6000$ reactions, including over $200$ components – varying from methane to hydrocarbons up to $C_{42}$.

CRACKSIM is a SEMK model developed at the Laboratory for Chemical Technology of the University of Ghent and contains over 1500 reactions.

In the current work, software tools such as SPYRO and CRACKSIM are not used for modelling naphtha cracking. The cracker model is developed in gPROMS ProcessBuilder and it uses kinetics from literature.

# Chapter 3

# Implementation

## 3.1 The gPROMS platform

gPROMS® is the software used in the development of the present work. It is the proprietary modelling platform of Process Systems Enterprise Ltd. (PSE), and is used for high-fidelity predictive modelling for the process industries. It is the foundation on which all of PSE's gPROMS family modelling and optimisation products are built.

Some of the most notable advantages of this custom modelling platform are the ability of building steady-state and dynamic process models of any complexity, and the simultaneous solving of all the equations in a model or flowsheet, making it a fast and robust environment

gPROMS ProcessBuilder® is the new product in the gPROMS family, having been released in 2015. Not only does it feature process flowsheeting capabilities and an extensive set of model libraries, but it also includes a custom modelling option, allowing for an easy drag-and-drop flowsheeting integration with custom models. This product was the main platform used for the present work, having been used for model development and flowsheeting, kinetic validation and furnace simulation.

## 3.2 Foreign Objects

gPROMS allows the usage of external software components, which provide certain additional computational services to gPROMS models and complement the already existing features. These are named Foreign Object (FO) and are defined as parameters in the model implementation. They include physical properties packages, external unit operation modules, or even complete computational fluid dynamics (CFD) software packages.

Three different FOs were used in the present work:

- Multiflash – physical property package;
- LSKM - responsible for the implementation of Large Scale Kinetic Mechanisms;
- ReadDataFO - used to supply external data to gPROMS, namely the molecular weight of all chemical species;

## 3.3 The Multiflash Software

Multiflash™ is a physical property package developed by Infochem Computer Services Ltd, mainly used for the study of fluids' physical properties and process simulation. It is accessible through a gPROMS interface and is licensed together with it as the standard property package.

On the graphical interface of Multiflash, the user defines all the components to be used, along with the physical property models selected. The resulting file (.mfl) is then imported into ProcessBuilder as a FO.

This package was used for kinetic testing and furnace simulation, having used the Redlich-Kwong-Soave (RKS) cubic equation of state as the thermodynamic model, due to its simplicity, robustness and efficiency and being especially appropriate for petrochemical applications [68]. The SuperTRAPP model was used to provide the transport properties, namely viscosity and thermal conductivity.

This physical property package will be used in a comparison with other sources for thermodynamic properties, in Appendix A, to test its reliability as a source of physical property calculations.

## 3.4 Implementation of Large Scale Kinetic Mechanisms

The implementation of the mechanistic kinetic models presents a few challenges, such as the modelling of the radical species involved, the uncertainty in the determined kinetic parameters, and the size of the scheme/problem (number of species and reactions), represented by stoichiometric matrices (reactions × species). The latter is the focus on this section of the work, since its optimisation brings great advantages to modelling by reducing the computing time.

To solve this problem, two approaches can be considered: reducing the number of chemical species and reactions, which is achievable by lumping, as discussed in the previous chapter, and will be further studied in Chapter 5; and the implementation of Large Scale Kinetic Mechanisms (LSKM), in which the objective is to pack the stoichiometric matrices by eliminating the zero elements.

This FO was developed by Tewardson [39] and takes advantage of the fact that the stoichiometric coefficient matrix is sparse (most of the elements in it are zero). This allows for the matrix to be compressed significantly, only including the non-zero values alongside with the necessary indexing information. There are several advantages in using this compression scheme:

- The compressed matrix takes up much less space in the computer memory;
- Getting data from the matrix in its compressed form is much easier and quicker;
- Only non-trivial operations are performed, saving a substantial amount of computing time;

### 3.4.1 Sparse matrix compression method

In this scheme, the data contained in the matrix is stored in three arrays: VE, RI and CIP. VE contains all the non-zero values of the matrix, while RI and CIP are used to extract the positions these values occupy in the matrix.

- VE (Value of Elements): length of the number of non-zero elements, only stores the non-zero values of the matrix;
- RI (Row Indices): length of VE, stores the row index of the corresponding element in VE. For a given $VE(x)$, $RI(x)$ stores the row where the value from VE is located in the original uncompressed matrix;
- CIP (Column Index Pointer): length of the number of columns, stores the position in which the non-zero element appears for each column. If the first non-zero element of the $y^{th}$ column is in position $k$ then$CIP(y) = k$.

To give an example of the compression method, matrix $M$ will be compressed into the three arrays:

$$M = \begin{bmatrix} 0 & b & d & 0 & g \\ a & c & 0 & 0 & 0 \\ 0 & 0 & 0 & 0 & h \\ 0 & 0 & e & 0 & 0 \\ 0 & 0 & 0 & f & 0 \end{bmatrix} \tag{3.1}$$

$$VE = [a \quad b \quad c \quad d \quad e \quad f \quad g \quad h] \tag{3.2a}$$

$$RI = [2 \quad 1 \quad 2 \quad 1 \quad 4 \quad 5 \quad 1 \quad 3] \tag{3.2b}$$

$$CIP = [1 \quad 2 \quad 4 \quad 6 \quad 7] \tag{3.2a}$$

In this example, the original matrix $M$ has size $5 \times 5$, storing 25 elements. With the application of the reduction scheme, it is possible to store the same amount of information in three arrays of lengths $8$, $8$ and $5$, adding up to 21 elements. Note that for this small matrix the application of the reduction scheme does not bring relevant results, but when dealing with larger sparse matrices (with thousands of elements), the benefits of using this compression method are immediately noticeable.

### 3.4.2 LSKM preparation and application

When imported into ProcessBuilder®, the LSKM FO is composed of two different .$txt$ files, one containing the data about the species involved in the reaction mechanism, and another one containing the data regarding the reactions: enthalpy of formation, forward and backwards pre-exponential factors and activation energy, as well as the species involved in each reactions, their stoichiometric coefficients and reaction orders. These files will be referred as *SpeciesFile* and *ReactionFile*, respectively, and are prepared in an Excel file, which includes the following sheets:

- Species: lists the species (and their molecular weight) that take part in the scheme, and attributes each one a Species_ID.

| | A | B | C |
|---|---|---|---|
| 1 | Species_ID | Species_Name | Molecular Weight [g/mol] |
| 2 | 1 | H2O | 18,01528 |
| 3 | 2 | H2 | 2,0158 |
| 4 | 3 | CH4 | 16,0426 |
| 5 | 4 | C2H4 | 28,0536 |
| 6 | 5 | C2H6 | 30,0694 |
| 7 | 6 | C3H6 | 42,0804 |
| 8 | 7 | C3H8 | 44,0962 |
| 9 | 8 | BDE13 | 54,0914 |
| 10 | 9 | C4H8_1 | 56,1072 |
| 11 | 10 | C4H8_2 | 56,1072 |
| 12 | 11 | iC4H8 | 56,1072 |

Figure 3.1 - Species sheet of the LSKM Excel file.

- LSKM input: lists the reactions present in the scheme, supplying all the data regarding the thermodynamic and kinetic parameters (reaction enthalpy, pre-exponential factors, activation energy) and the species involved in each reaction (stoichiometric coefficients and reaction order) by each species' ID.

| | A | B | C | D | E | F | G | H | I | J | K | L | M | N | O | P | Q | R | S | T | U | V | W | X | Y |
|---|---|---|---|---|---|---|---|---|---|---|---|---|---|---|---|---|---|---|---|---|---|---|---|---|---|
| 1 | | | Forward | | Backwards (**) | | | | | | | | | | | | | | | | | | | | |
| 2 | Reactions | Reaction enthalpy [kcal/mol] | Pre-exponential factors | Activation energy | Pre-exponential factors | Activation energy | no_ species involved | **IDs** of species involved | | | | | | **Stoichiometric coefficients** of species involved | | | | | | **Orders (***)** for species involved | | | | | |
| 3 | 1 | 0 | 17,70 | 84,16 | 0 | 0 | 3 | 13 | | 40 | 45 | | | -1 | | 1 | 1 | | | 1 | | 0 | 0 | | |
| 4 | 2 | 0 | 17,79 | 85,46 | 0 | 0 | 3 | 18 | | 40 | 46 | | | -1 | | 1 | 1 | | | 1 | | 0 | 0 | | |
| 5 | 3 | 0 | 17,10 | 81,56 | 0 | 0 | 3 | 18 | | 42 | 44 | | | -1 | | 1 | 1 | | | 1 | | 0 | 0 | | |
| 6 | 4 | 0 | 17,50 | 83,96 | 0 | 0 | 3 | 19 | | 40 | 47 | | | -1 | | 1 | 1 | | | 1 | | 0 | 0 | | |
| 7 | 5 | 0 | 16,90 | 80,07 | 0 | 0 | 3 | 19 | | 42 | 45 | | | -1 | | 1 | 1 | | | 1 | | 0 | 0 | | |
| 8 | 6 | 0 | 17,40 | 85,36 | 0 | 0 | 3 | 19 | | 40 | 48 | | | -1 | | 1 | 1 | | | 1 | | 0 | 0 | | |
| 9 | 7 | 0 | 16,80 | 81,86 | 0 | 0 | 3 | 26 | | 42 | 46 | | | -1 | | 1 | 1 | | | 1 | | 0 | 0 | | |
| 10 | 8 | 0 | 16,50 | 81,86 | 0 | 0 | 2 | 26 | | 44 | | | | -1 | | 2 | | | | 1 | | 0 | | | |
| 11 | 9 | 0 | 17,10 | 82,86 | 0 | 0 | 3 | 27 | | 40 | 51 | | | -1 | | 1 | 1 | | | 1 | | 0 | 0 | | |
| 12 | 10 | 0 | 16,60 | 79,17 | 0 | 0 | 3 | 27 | | 44 | 45 | | | -1 | | 1 | 1 | | | 1 | | 0 | 0 | | |

Figure 3.2 - LSKM input sheet of the LSKM Excel file.

- Control: Generates the .$txt$ files from the previous two sheets.

After setting the Excel file, the FO now contains all the information needed regarding the used reaction scheme.

For definition of the size of the problem, the following integer scalar outputs are generated:

- NoSpecies: total number of species;
- NoReactions: total number of reactions;
- NoStoichCoeffs: total number of non-zero stoichiometric coefficients;
- NoReactants: total number of species acting as reactants in forward reactions;
- NoProducts: total number of species acting as products in forward reactions;

For the stoichiometric matrix of $r$ rows of reactions and $s$ columns of species the following arrays are generated:

- ReactionSC($k$): size of NoReactions, contains the values of the non-zero stoichiometric coefficients stored in the matrix;
- ReactionID($k$): size of NoReactions, returns the reaction for the stoichiometric coefficient in ReactionSC($k$);
- SpecStartAddress($s$): size of NoSpecies, returns the position of the first non-zero stoichiometric coefficient of each species $s$ in ReactionSC.

The following arrays are also generated based on the matrix, but contain data regarding the reaction order:

- ForwardReactionOrder($k$): size of NoReactants, contains the values of the non-zero reaction orders of each species $s$ in each of the forward reactions $r$;
- ReactionID_reactant($k$), size of NoReactants, returns the reaction, $r$, for the reaction order in ForwardReactionOrder($k$);
- ReactantStartAddress($s$), size of NoReactions, stores the value where the reaction orders for the component $s$ start in the ForwardReactionOrder array.
- BackwardsReactionOrder($k$): size of NoProducts, stores the values of the non-zero reaction order of each species $s$ in each the backwards reactions $r$;
- ReactionID_product($k$), size of NoProducts, returns the reaction, $r$, for the reaction order in BackwardsReactionOrder($k$);
- ProductStartAddress($s$), size of NoReactions, stores the value where the reaction orders for the component $s$ start in the BackwardsReactionOrder array.

Finally, the kinetic parameters are stored in the following arrays:

- ForwardPreExponentialFactor() size of NoReactions, contains the forward pre-exponential factors for each reaction;
- ForwardActivationEnergy() size of NoReactions, contains the activation energy for each reaction;
- BackwardsPreExponentialFactor() size of NoReactions, contains the backwards pre-exponential factors for each reaction;
- BackwardsActivationEnergy() size of NoReactions, contains the activation energy for each reaction;

# Chapter 4

# Steam cracking furnace

The focus of this chapter is to describe the models used in this work, namely the ones that are essential parts of the cracking furnace and the connections between these models, as well as showing the process of modelling a new coil, which will be used for simulation and optimisation in Chapter 5.

The basic schematic representation of the structure of the furnace model is as showed in the Figure 4.1.

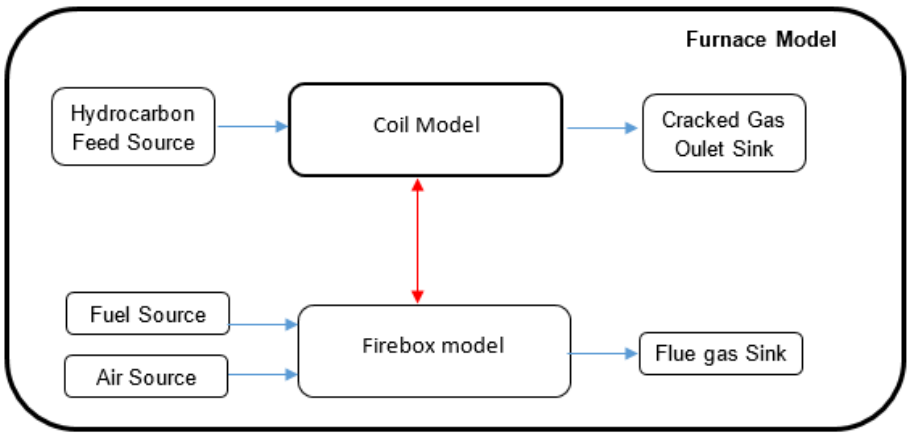


Figure 4.1 - Schematic of the models and connections in the cracking furnace.

Material connections are shown in blue, while connections regarding flux of energy/heat (distributed thermal contact) are shown in red.

In the next section of the work, each of these models will further studied, detailing the main equations that define each of one of them, as well as the purpose of the model. The coil model will be studied with greater detail, as it represents the heart of furnace, and where the cracking reactions take place, making it the most crucial model for this work.

## 4.1 Model equations

This section of the work has the focus of doing an overview of the most important models that constitute the cracking furnace (as seen in Figure 4.1), by detailing the purpose of each model and going over the main equations (mass, energy and momentum balance) that define such models.

The models reviewed in this section are “generic” models that are already implemented into the general libraries of gPROMS, and that will serve as a foundation for the development of custom models, adapted to specific requirements of the current work, in subchapter 4.2 and Chapter 5.

### 4.1.1 Source and Sink models

These models are part of the gML (gPROMS Modelling Libraries), developed by PSE. These are two of the most used models, since they define the conditions from the inlet and outlet of a specified flowsheet.

The Source model is used for defining the material stream entering the flowsheet. The user may define the phases present (liquid, vapour or two phase), as well as assigning variables such as temperature, pressure and flow and composition. It is into this model that the FO Multiflash is imported, providing the physical properties for the specified components.

The Sink model is used for defining the material stream exiting the flowsheet. In the current work, there weren’t any specifications to be made, but variables like pressure, temperature or mass fraction can be specified, in cases of flow reversal.

### 4.1.2 Coil/Tube model

In the furnace, the radiant coil can have many different configurations, ranging from being composed of only one tube associated with one energy input model to several tubes associated in series and/or parallel, with the same number of energy input models. The decision of the configuration of the tubes is made based upon the gathered information of the coil.

Since each tube is modelled in the same way, the focus of this chapter is to review the tube model, as well as its constituting sub-models, which are:

- Fluid properties model;
- Heat transfer coefficient model;
- Friction factor coefficient model;
- Kinetic model

These sub-models are independent and can be used outside the tube model, in other higher-level models. With the integration of these sub-models into the main tube model allows the latter to fully describe all phenomena occurring in the tube, from heat transfer to cracking reactions.

The tube model, in itself, contains the equations of mass, energy and momentum balance, that allow it to describe such phenomena inside of the tube. These equations are briefly described in the next section.

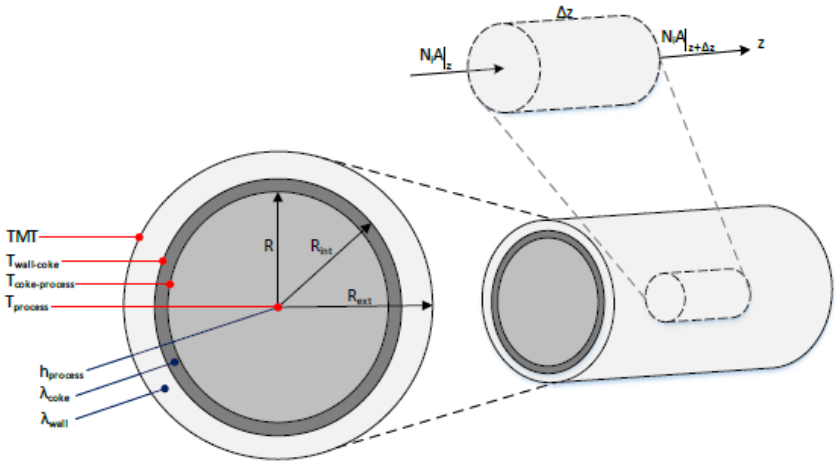


Figure 4.2 - Schematic of a tube cross section area and differential volume control.

The cross sectional area of the tube can vary along the tube, due to the deposition of coke across the reactor length, which causes the radius $R$ to decrease, making $A(z) = \pi R(z)^2$ decrease as well alongside the reactor length.

Due to the turbulent nature of the flow inside the tube (high Reynolds number) and the low viscosity, the tube will be treated as plug-flow reactor (PFR) the radial contribution of the flux can be neglected, making the mass balance being represented by the following equation:

$$\frac{d}{dz}[N_i(z)A(z)] = MW_i A(z) r_i(z) \tag{4.1}$$

Where $N_i$ represents the mass flux for component $i$, $A$ is the cross-section area of the tube, $MW_i$ is the molecular weight of component $i$ and $r_i$ is the overall reaction rate (rate of formation/disappearance) of component $i$.

The energy balance can be described by the following equation:

$$\frac{d}{dz}[q(z)A(z)] = q_{ext}(z) 2\pi R_{ext} \tag{4.2}$$

Where $q(z)$ represents the heat flux and $R_{ext}$ represents the outside radius of the tube, through which the heat flux $q_{ext}$ is exchanged.

The momentum balance (associated with pressure drop) can be described by the following equation:

$$\frac{d}{dz}[P(z)A(z)] = -N_{total}(z)A(z)\frac{dv(z)}{dz} - \frac{v(z)^2 A(z)\rho(z)}{2}\left(\frac{2f_{Fanning}}{R(z)} + \frac{n_B f_{bend}(z)}{L}\right) \quad (4.3)$$

where $P$ is the pressure of the process stream, $N_{total}$ is the total mass flux, $v$ and $\rho$ the linear velocity and density of the process stream, $f_{Fanning}$ is the Fanning friction factor and $n_B$ and $f_{bend}$ are the number and friction factor of the bends.

#### 4.1.2.1 Fluid properties model

This model has the purpose of making all calculations regarding the physical properties of the fluids in the tube, like density, enthalpy, heat capacity, viscosity and thermal conductivity.

In most cases, an external physical property package (like Multiflash) is used to calculate most of the properties, expect for concentrations and gas density, which are calculated within this model, according the ideal gas law. Moreover, the kinetic scheme used is a radical one, and since Multiflash does not have support for radical species, all properties for the radical species are calculated in this fluid property model.

#### 4.1.2.2 Heat transfer coefficient model

This model contains correlations regarding heat transfer that takes place in the tube. For this, the Dittus-Bolter correlation for turbulent flow was applied:

$$Nu(z) = 2.43 \times 10^{-2} Re(z)^{0.8} \mathrm{Pr}(z)^{0.4} \quad (4.4)$$

Which is applicable for $Reynolds > 1000$ and $0.7 < Prandtl < 170$. [40]

#### 4.1.2.3 Friction factor coefficient model

To calculate the friction factor in the tube, the Churchill equation was applied (for Re>4000) [29].

$$\frac{1}{\sqrt{f_{Fanning}}} = \log_{10}\left(\frac{\varepsilon}{3.7D} + \frac{7.0}{Re^{0.9}}\right) \quad (4.5)$$

In which $\varepsilon$ is the inner roughness of the tube.

To calculate the friction factor in the bend, the Nekrasov equation was applied [41]:

$$f_{bend} = \left(0.7 + 0.35\,\frac{\alpha_{bend}}{90}\right)\left(0.051 + 0.019\,\frac{2R(z)}{R_{bend}}\right) \quad (4.6)$$

In which $\alpha_{bend}$ and $R_{bend}$ are the angle and radius of the bend.

#### 4.1.2.4 Kinetic model

This model has the purpose of selecting the kinetic scheme to use (by choosing from an array of different types of schemes), and to calculate the forward ($f$) and backwards ($b$) rate constants ($k$), for each reaction $j$, using the Arrhenius equation:

$$k_j = \mathrm{k}_0\, e^{-\frac{Ea_j}{RT(z)}} \quad (4.7)$$

In which $\mathrm{k}_0$ represents the pre-exponential factor and $Ea_j$ the activation energy.

It can also calculate the reaction rate, $r_j$, for each reaction $j$:

$$r_{j(z)} = k_{f,j} \prod(C_{react}(z)) - k_{b,j} \prod(C_{prod}(z)) \quad (4.8)$$

Where $C_{react}$ represents the molar concentration of the reactants (for the forward reactions) and $C_{react}$ the molar concentration of the products (for the backwards reactions).

### 4.1.3 Energy input model

This model is responsible for specifying and/or determining the heat flux between the furnace burner and the cracking coils. It allows three different heat flux specifications:

- Specify the heat flux profile, and thus calculating the process gas temperature profile as a result;
- Impose the process gas temperature profile, and thus calculating the heat flux profile;
- Predict the heat flux profile;

When calculating the heat flux profile, the Stefan-Boltzmann law is employed, which relates the heat flux with the temperature of the flames, $T_{flame}$, and the temperature of the tube wall, $TMT$.

$$q_{ext}(z) = \varepsilon \cdot \sigma\left({T_{flame}}^4 - TMT^4\right) \quad (4.9)$$

## 4.2 Modelling of the naphtha cracking furnace

The focus of this section is to review the process of modelling a naphtha cracking furnace with a typical cracking coil, which will be used to simulate typical operation and to compare the model predictions to typical data.

This coil model is constructed using the existing model libraries in gPROMS ProcessBuilder.

### 4.2.1 Coil type

The goal of this simulation is to model a coil that accurately predicts and matches typical data for naphtha cracking units. A Naphtha cracker with a typical SRT VI (Short Residence Time) coil is selected for the model development. These cracking coils have short residence time ( ~ 0.22 sec) and operate at high heat fluxes (q> 100 KW/m2). The first pass of the coil consists of four parallel tubes which are then merged into a single second pass. [42]

### 4.2.2 Coil geometry and operating conditions

In order to be able to model the coil, it is necessary to gather information regarding the geometry of the coil (length, tube diameter, angle bends) and operating conditions, like typical values of flow rates, inlet and outlet temperature and pressure. After doing some research on literature regarding SRT-VI coils [42-44], it is possible to get a schematic representation of the coil and a summary of its most important operating conditions.

Figure 4.3 shows a schematic of a SRT-VI coil, while Table 4.1 shows typical operating conditions used with this type of coil.

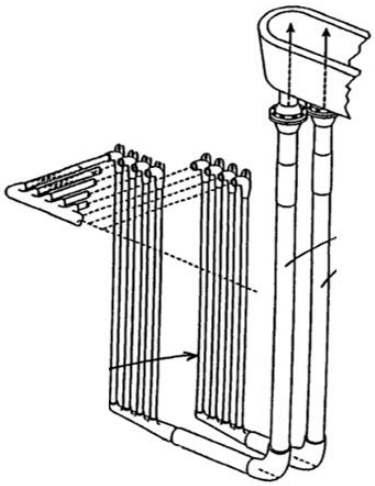

Figure 4.3 - Schematic of a SRT-VI two pass coil.

Table 4.1 - Operating Conditions for a SRT-VI coil.

| | Unit | [44] | [42] | [43] |
|---|---|---|---|---|
| Pass 1: inner diameter | $cm$ | 5.08 | - | - |
| Pass 1: outer diameter | $cm$ | 6.35 | - | - |
| Pass 1: number parallel tubes | | 16 | - | - |
| Pass 2: inner diameter | $cm$ | 10.16 | - | - |
| Pass 2: outer diameter | $cm$ | 11.43 | - | - |
| Pass 2: number parallel tubes | | 4 | - | - |
| Length of pass | $m$ | 9.144 | - | - |
| Hydrocarbon flow | $tonne/h$ | 4.00 per coil | 37.9 per furnace | - |
| Residence time | $s$ | - | 0.22 | 0.40 |
| Steam:Oil ratio | | 0.5 | - | - |
| Inlet temperature | ℃ | 621.1 | - | - |
| Coil outlet temperature | ℃ | 833.3 | - | 850 |
| Coil outlet pressure | $bar\ abs$ | - | - | 1.70 |
| Pressure drop | $bar$ | 0.1103 | - | - |
| Maximum wall temperature | ℃ | 1068.9 | - | - |
| Firebox temperature | ℃ | 1185 | - | - |
| Pass 1: Heat transfer coefficient | $W/m^2$ | 191.17 | - | - |
| Pass 2: Heat transfer coefficient | $W/m^2$ | 177.92 | - | - |
| External heat transfer area | $m^2$ | 42.317 | - | - |

Based on the figure and table presented above, it was decided to model the coil with four-to-one configuration of tubes, in which four smaller diameter tubes ($d = 5.08\ cm$) converge into one tube ($d = 10.16\ cm$). The length of each pass was also considered to be $9.15\ m$, as found in literature. However, in order to get a more realistic approach and model the plant coil as accurately as possible, a new horizontal pass was added between passes 1 and 2, as well as 2 adiabatic sections, at the start of pass 1 (pass 0) and at the end of pass 2 (pass 2a), as shown in the Figure 4.4.

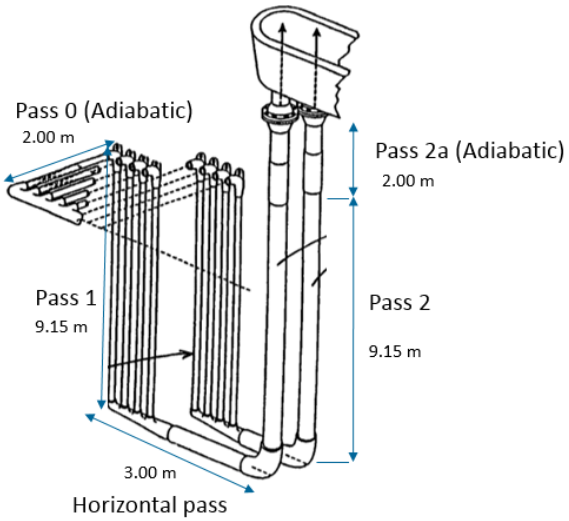


Figure 4.4 - Schematic of the modelled SRT-VI coil.

Table 4.2 shows the geometry details used for the modelled coil, and Table 4.3 shows main operating conditions for the furnace, which will be further analysed in chapter 5.

Table 4.2 - Geometry details for the modelled coil.

| Geometry parameter | Unit | Pass 0 | Pass 1 | Horizontal pass | Pass 2 | Pass 2a |
|---|---|---|---|---|---|---|
| Number of parallel tubes | | 4 | 4 | 1 | 1 | 1 |
| Inner diameter | $cm$ | 5.08 | 5.08 | 10.16 | 10.16 | 10.16 |
| Outer diameter | $cm$ | 6.35 | 6.35 | 11.43 | 11.43 | 11.43 |

The tube wall thickness is the same for every pass of the coil, at $0.635\ cm$

Table 4.3 - Operating conditions for the modelled furnace.

| Furnace operating conditions | Unit | |
|---|---|---|
| Number of coils | | 24 |
| Naphtha feed rate | $tonne/h$ | 36.0 |
| Steam:Oil ratio | | 0.50 |
| Residence time | $s$ | 0.22 |
| CIT | ℃ | 620 |
| COT | ℃ | 835 |
| COP | $bar\ abs$ | 1.70 |

It is worth mentioning that furnace was modelled with 24 coils (Figure 4.4 displays 2 coils) so that, given the flowrate, the residence time was set to $0.22\ s$ and a turbulent flow was kept inside the tube.

After defining all the geometry parameters and operating conditions, the models for the SRT-VI coil and furnace can be built. The following figures show the flowsheet for the coil and furnace models.

The furnace model (Figure 4.5) includes the source models HC, for hydrocarbon feed, and Steam, as well as a Sink model, all reviewed in section 4.1.1. The coil model is externally connected to the furnace through material and energy ports.

For the coil model (Figure 4.6) it is to note that all passes are built using the same tube model, whose equations have been described in section 4.1.2. The models FM_1 and FM_2 represent flow multipliers, which are responsible for the branching of the material flow: dividing the flow before pass 1 (which has 4 parallel tubes) and converging it into a single tube for the horizontal pass (pass_h), as seen in figure 4.4. The energy_input models had their basic structure reviewed in section 4.1.3. It is noteworthy that the heat flux for passes 0 and 2a are set to zero, since those are adiabatic sections.

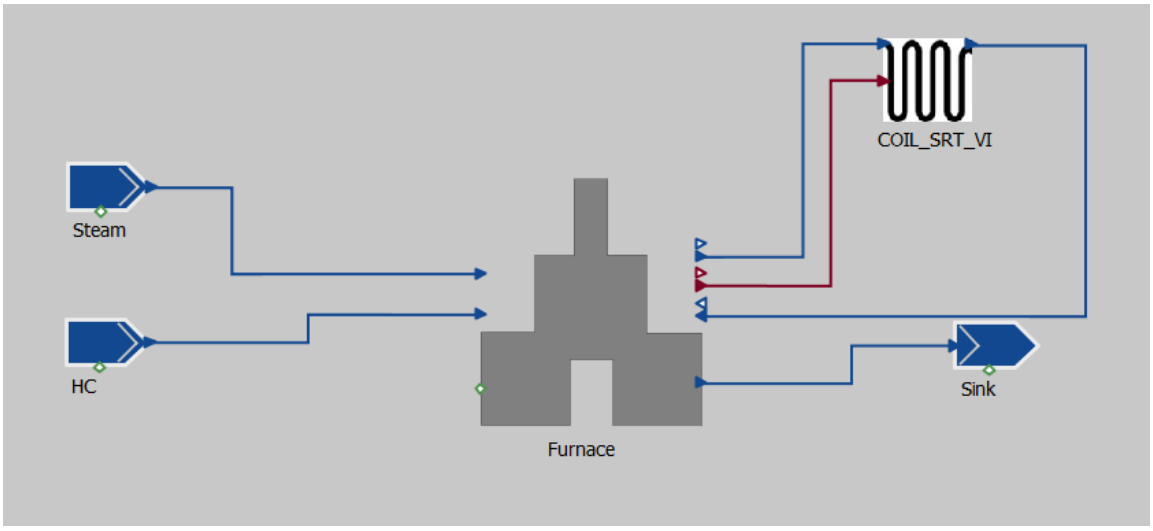


Figure 4.5 - Flowsheet of the furnace model.

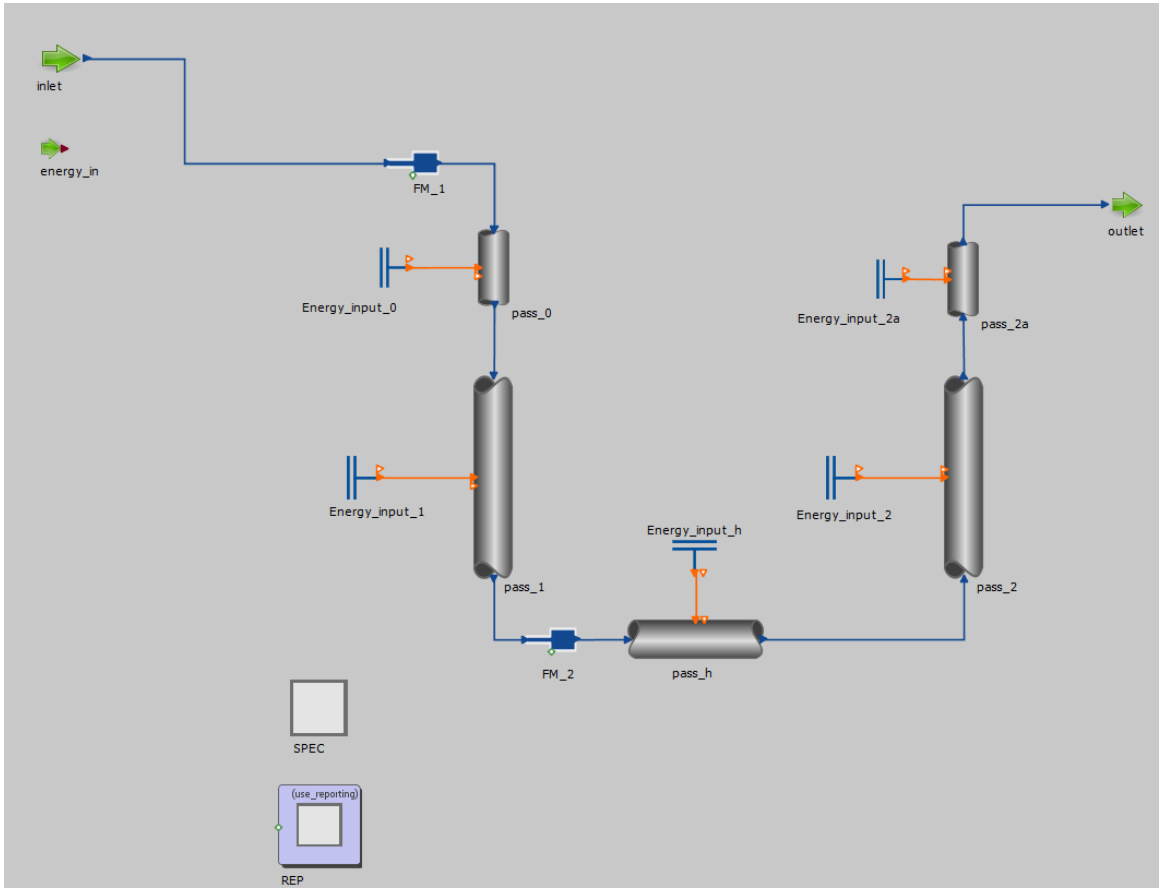


Figure 4.6 - Topology of the SRT-VI coil model.

# Chapter 5

# Furnace simulation and kinetic tuning

This chapter will focus on the simulation study for the modelled furnace, with the objective of trying to predict and match the typical data for the cracking of naphtha. (Appendix C)

In order to accurately match typical data for naphtha cracking, the simulation results will have to give reasonable predictions for the yields of the most relevant olefins (ethylene, propylene, butadiene), but it will also have to match conversion for the main elements present in the naphtha feed. For that reason, the kinetic mechanisms used for the simulation will have to include the highest number possible of the components that are present in the feed.

First, in section 5.1, the kinetic mechanisms will be reviewed, to assess if they include the components of interest, and to set up a lumping procedure to include the components that are not present.

In the next section 5.2 the work will focus on doing a simulation study with the modelled furnace, using the chosen kinetics, and performing some sensitivity analysis of the main operating conditions.

Finally, in section 5.3 the work will focus on performing kinetic tuning, with the objective of accomplishing better predictions, the kinetic mechanisms will be manually tuned, by adding components and reactions from other sources, as well as the tuning of the kinetic parameters.

## 5.1 Component Lumping

In this section of the work, the component list for feed and product in typical data for naphtha cracking furnaces is compared with the component list from the various kinetic mechanisms. In order to try to as accurately as possible match the typical data, the components which are not part of the kinetic schemes will be lumped with already existing components. This procedure will be reviewed in section 5.1.2.

## 5.1.1 Comparison of the kinetic schemes

As previously said in Chapter 2, for naphtha cracking, the radical kinetic mechanisms result in better predictions of the yields of olefins. From the available kinetics, the schemes from Joo [20] [22] and Towfighi [19] [35] were chosen for this work.

Table 5.1 shows the comparison of the components of interest and their presence in the kinetic schemes from literature.

Table 5.1 - Components comparison between typical data and kinetic schemes.

| | **Typical Data** | **Joo** | **Towfighi** |
|---|---|---|---|
| Feed: Number of components | 24 | 17 | 19 |
| Feed: % of components | - | 81.6 | 85.8 |
| | | | |
| Products: Number of components | 97 | 38 | 35 |
| Products: % of components | - | 89.6 | 86.1 |

It can be seen that the chosen kinetic mechanisms do not include all the components that are present in the naphtha feed and product. It is most noticeable for the products, in which only $38$ or $35$ components are represented, out of 97. However, the components that are not present make up $10.4\%$ and $13.9\%$ of the product composition, which is somewhat manageable by means of component lumping.

In the next section, component lumping will be applied so that the feed composition of naphtha can be reproduced and that all products of the cracker are included in the kinetic schemes.

## 5.1.2 Lumping of the components

The objective of this procedure is to group components into an equivalent or pseudo component, with similar physical properties, and that would reacts in a similar manner, if added to a pyrolysis reaction. [46] [47]

For the lumping of components, some rules will be defined, in order to perform the lump in the same way for the different reaction schemes.

- Isomers will be lumped into another isomer (1,3-Hexadiene → 1,4-Hexadiene);
- Branched alkanes/alkenes will be lumped into the closest linear alkane/alkene, maintaining the number of carbon atoms;
- Heavy components will be lumped into the heaviest component present in the scheme, taking into account its type (linear alkanes, cycloalkanes and aromatics).

The following tables present components that are not in the kinetic schemes, their weight percentage and the component they were lumped into in each of the schemes (components that are already in one of the schemes are not lumped, and shown as – in the table).

Table 5.2 - Component lumping for the feed.

| Component | wt. % | Joo | Towfighi |
|---|---|---|---|
| Ethyl-Benzene | 0.39 | Toluene | - |
| C7-NAF [1] | 6.21 | methyl-cyclohexane | cycloheptene |
| C8-NAF [2] | 4.67 | methyl-cyclohexane | cyclooctane |
| i-nonane | 3.31 | n-nonane | - |
| C8-NAF [3] | 2.44 | methyl-cyclohexane | Isopropyl-cyclohexane |
| C9-ARO [4] | 0.52 | Xylene | |
| n-decane | 0.18 | n-nonane | |
| i-decane | 0.68 | n-nonane | i-nonane |

Table 5.3 - Component lumping for the products.

| Component | wt. % | Joo | Towfighi |
|---|---|---|---|
| Acetylene | 0.003 | Ethylene | - |
| Propadiene | 0.64 | Propylene | |
| vynil-acetylene | 0.04 | 1,3-butadiene | |
| 2-butene | 1.03 | - | 1-butene |
| i-butene | 2.91 | - | |
| cyclopentadiene | 1.54 | Cyclopentane | |
| 1,3- / 1,4-pentadiene | 0.49 | 1-pentene | |
| isoprene | 0.64 | 3-methyl-1-butene | 1,3-butadiene |
| cyclopentene | 0.33 | cyclopentane | |
| 2-pentene | 0.14 | - | 1-pentene |
| 2-methyl-1-butene | 0.25 | 3-methyl-1-butene | |
| 2-methyl-2-butene | 0.05 | | |
| 3-methyl-1-butene | 0.10 | - | |
| methyl-cyclopentadiene | 0.40 | methyl-cyclopentane | |
| 2-methyl-1,3-Pentadiene | 0.29 | 1-hexene | 1-pentene |
| methyl-cyclopentene | 0.10 | methyl-cyclopentane | |
| 1-hexene | 0.04 | - | 1-pentene |
| 2- / 3-hexene | 0.003 | - | |
| C6 olefins | 0.06 | 1-hexene | |
| C7-NAF | 0.16 | methyl-cyclohexane | cycloheptene |
| methyl-cyclohexene | 0.06 | | |
| 1-heptene | 0.01 | - | 1-pentene |
| C7 olefins | 1.54 | 1-heptene | |
| Styrene | 0.60 | - | Toluene |
| 1-Octene | 0.003 | 1-heptene | 1-pentene |
| C8 Olefins | 0.01 | | |
| C8-NAF | 0.04 | methyl-cyclohexane | cyclooctane |
| i-Nonane | 0.02 | n-nonane | - |
| C9-NAF | 0.01 | methyl-cyclohexane | Isopropyl-cyclohexane |
| C9-ARO | 0.14 | Xylene | |
| Methyl-Styrene | 0.33 | Xylene | |
| Indene | 0.27 | | |
| Naphthalene | 0.90 | | |
| >C10 Olefins | 0.30 | n-heptene | n-pentene |
| >C10 Aromatics | 0.20 | Xylene | |

1- Naphthenic C7;
2- Naphthenic C8;
3- Naphthenic C9;
4- Alkyl-aromatic component with 9 carbon atoms.

## 5.2 Simulation of the naphtha cracking furnace

After performing the components lumping, it is now possible to reproduce the naphtha feed to the cracker and simulate the furnace to try to predict and match typical data for naphtha cracking furnaces

Two different cases were run, using with the two different kinetic schemes. The operating conditions are shown in table 5.4.

Table 5.4 - Operating conditions for the real naphtha cracking furnace.

| Furnace operating conditions | Unit | |
|---|---|---|
| Naphtha feed rate | $tonne/h$ | 36.0 |
| Steam:Oil ratio | | 0.50 |
| Residence time | $s$ | 0.22 |
| CIT | ℃ | 620 |
| COT | ℃ | 835 |
| COP | $bar\ abs$ | 1.70 |

The feed composition, the comparison between typical yield data and simulation results for yields and conversion is shown in tables 5.5 and 5.6, for the cases of using the kinetics of Towfighi and Joo, respectively.

Table 5.5 - Simulation results and comparison with typical yields for the Towfighi kinetic scheme.

| Components | Feed Compositon (wt. %) | | Typical data yield (%) | Simulation yield (%) | yield dev. | yield dev. (%) | | Typical data conversion (%) | Simulation conversion (%) |
|---|---|---|---|---|---|---|---|---|---|
| Hydrogen | 0 | | 0.87 | 0.25 | -0.6 | -71% | | - | - |
| Methane | 0 | | 14.36 | 9.64 | -4.7 | -33% | | - | - |
| **Ethylene** | 0 | | **27.62** | **21.60** | **-6.0** | **-22%** | | - | - |
| Ethane | 0 | | 3.53 | 0.10 | -3.4 | -97% | | - | - |
| **Propylene** | 0 | | **17.51** | **6.75** | **-10.8** | **-61%** | | - | - |
| Propane | 0 | | 0.48 | 0.01 | -0.5 | -99% | | - | - |
| n-butane | 6.64 | | 1.35 | 0 | -1.3 | -100% | | 79.6 | 100 |
| 1-butene | 0 | | 5.77 | 0.03 | -5.7 | -99% | | - | - |
| **1,3-butadiene** | 0 | | **5.70** | **6.07** | **0.4** | **6%** | | - | - |
| n-pentane | 11.48 | | 1.10 | 6.32 | 5.2 | 476% | | 90.4 | 45.0 |
| i-pentane | 9.78 | | 0.97 | 1.66 | 0.7 | 72% | | 90.1 | 83.1 |
| n-hexane | 9.13 | | 0.48 | 3.93 | 3.4 | 718% | | 94.7 | 57.0 |
| i-hexane | 10.83 | | 0.43 | 0.89 | 0.5 | 110% | | 96.1 | 91.8 |
| Benzene | 0.61 | | 5.61 | 0.98 | -4.6 | -83% | | - | - |
| Toluene | 1.52 | | 3.67 | 1.52 | -2.1 | -58% | | - | - |
| Xylene | 2.31 | | 2.80 | 2.31 | -0.5 | -18% | | - | - |
| n-heptane | 5.31 | | 0.15 | 2.28 | 2.1 | 1398% | | 97.1 | 57.0 |
| i-heptane | 7.79 | | 0.17 | 0.59 | 0.4 | 255% | | 97.9 | 92.5 |
| Cycloheptane | 6.21 | | 0.22 | 6.28 | 6.1 | 2732% | | - | - |
| n-octane | 4.12 | | 0.07 | 4.12 | 1.0 | 6192% | | - | - |
| i-octane | 6.39 | | 0.08 | 6.39 | 6.3 | 8257% | | - | - |
| Cyclooctane | 4.67 | | 0.04 | 4.67 | 4.6 | 11986% | | - | - |
| n-nonane | 2.10 | | 1.87 | 2.10 | 0.2 | 13% | | - | - |
| i-nonane | 3.99 | | 0.02 | 3.99 | 3.9 | 15870% | | - | - |

Table 5.6 - Simulation results and comparison with typical yields for the Joo kinetic scheme.

| Components | Feed Composition (wt. %) | | Typical data yield (%) | Simulation yield (%) | yield dev. | yield dev. (%) | | Typical data conversion (%) | Simulation conversion (%) |
|---|---|---|---|---|---|---|---|---|---|
| Hydrogen | 0 | | | 0.27 | -0.6 | -69% | | - | - |
| Methane | 0 | | 14.36 | 9.12 | -5.2 | -36% | | - | - |
| **Ethylene** | 0 | | **27.96** | **25.91** | **-2.1** | **-7%** | | - | - |
| Ethane | 0 | | 3.53 | 3.72 | 0.2 | 5% | | - | - |
| **Propylene** | 0 | | **17.51** | **19.70** | **2.2** | **12%** | | - | - |
| Propane | 0 | | 0.48 | 0 | -0.5 | -100% | | - | - |
| n-butane | 6.64 | | 1.35 | 0.35 | -1.0 | -74% | | 79.6 | 94.7 |
| 1-butene | 0 | | 1.83 | 11.95 | 10.1 | 552% | | - | - |
| **1,3-butadiene** | 0 | | **5.05** | **4.64** | **-0.5** | **-8%** | | - | - |
| i-butene | 0 | | 2.91 | 1.17 | -1.7 | -60% | | - | - |
| n-pentane | 11.48 | | 1.10 | 2.15 | 1.1 | 96% | | 90.4 | 80.9 |
| i-pentane | 9.78 | | 0.97 | 1.08 | 0.1 | 12% | | 90.1 | 88.7 |
| n-hexane | 9.13 | | 0.48 | 3.77 | 3.3 | 687% | | 94.7 | 57.8 |
| i-hexane | 10.83 | | 0.43 | 1.35 | 1.0 | 218% | | 96.1 | 87.3 |
| methyl-cyclohexane | 13.32 | | 0.27 | 0.08 | -0.2 | -90% | | - | - |
| Benzene | 0.61 | | 5.61 | 0.60 | -5.0 | -89% | | - | - |
| Toluene | 1.91 | | 3.67 | 1.87 | -1.8 | -49% | | - | - |
| Xylene | 2.31 | | 2.80 | 2.26 | -0.5 | -19% | | - | - |
| n-heptane | 5.31 | | 0.15 | 0 | -0.2 | -100% | | 97.1 | 100 |
| i-heptane | 7.79 | | 0.17 | 0 | -0.2 | -100% | | 97.9 | 100 |
| n-octane | 4.12 | | 0.07 | 0 | -0.1 | -100% | | - | - |
| i-octane | 6.39 | | 0.08 | 0 | -0.1 | -100% | | - | - |
| n-nonane | 6.10 | | 1.87 | 5.98 | 4.1 | 220% | | - | - |

It is noteworthy that the feed composition is slightly different for the two cases, since the same component in the feed can be lumped into a different component for each kinetic scheme, since the two don't share the same list of components.

Analysing the two sets of simulations, it is clear that the simulations using the Joo kinetic scheme produce much better predictions than those using Towfighi, in terms of the yields of the light olefins (ethylene, propylene), as well as the conversion of the main components found in the naphtha feed (pentane and hexane). There are, however, still some components which are not being well predicted, such as the aromatics. In order to solve this, section 5.3 will focus on kinetic tuning.

## 5.2.1 Sensitivity analysis

Before kinetic tuning, a sensitivity analysis will be performed on one of the operating conditions, the Coil Outlet Temperature, ($COT = 835℃$ during the initial simulation), as it is a variable which greatly affects the performance of cracking furnace.

This variable will vary between $830℃$ and $845℃$, and the yields of the main olefins and the conversion of the main components in the feed will be analysed.

Table 5.7 - Sensitivity analysis of COT on the yields and conversions.

| Components | Simulation yield (%) | Case 1 yield (%) | Case 2 yield (%) | Case 3 yield (%) | Simulation conversion (%) | Case 1 conversion (%) | Case 2 conversion (%) | Case 3 conversion (%) |
|---|---|---|---|---|---|---|---|---|
| Hydrogen | 0.27 | 0.26 | 0.27 | 0.28 | - | - | - | - |
| Methane | 9.12 | 8.08 | 9.28 | 9.71 | - | - | - | - |
| Ethylene | 25.91 | 25.08 | 26.32 | 27.44 | - | - | - | - |
| Propylene | 19.70 | 19.55 | 19.76 | 19.9 | - | - | - | - |
| n-butane | 0.35 | - | - | - | 94.7 | 94.2 | 95.1 | 95.5 |
| 1,3-butadiene | 4.64 | 4.36 | 4.77 | 5.16 | - | - | - | - |
| n-pentane | 2.15 | - | - | - | 80.9 | 77,4 | 84,1 | 87,0 |
| i-pentane | 1.08 | - | - | - | 88.7 | 85,9 | 91,1 | 93,1 |
| n-hexane | 3.77 | - | - | - | 57.8 | 55,0 | 60,7 | 63,5 |
| i-hexane | 1.35 | - | - | - | 87.3 | 84,6 | 89,7 | 91,7 |
| n-heptane | 0 | - | - | - | 100 | 100,0 | 100,0 | 100,0 |
| i-heptane | 0 | - | - | - | 100 | 100,0 | 100,0 | 100,0 |

1- $COT = 830℃$
2- $COT = 840℃$
3- $COT = 845℃$

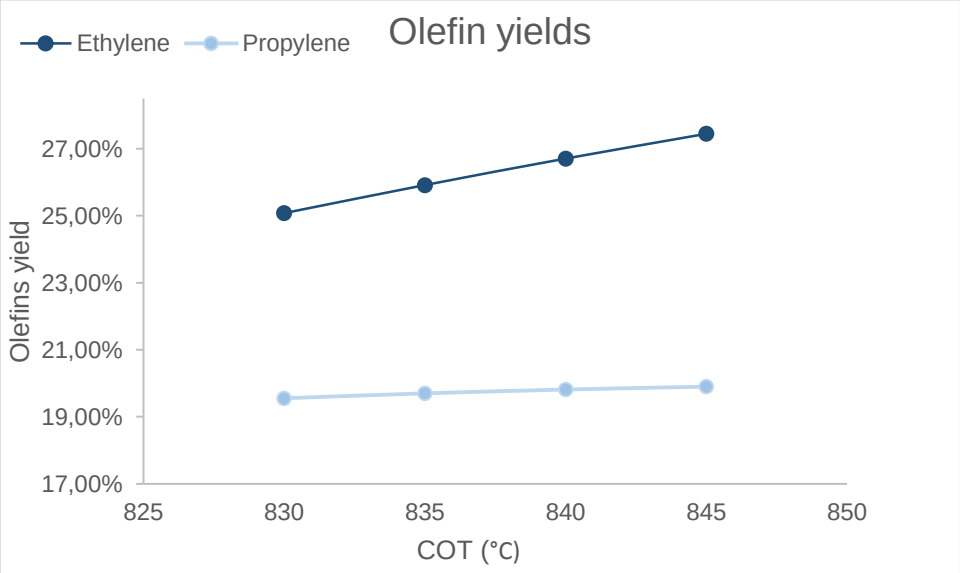


Figure 5.1 - Sensitivity analysis of COT on yields of olefins.

From analysing these results, one can conclude that the yield of ethylene and propylene has a slight with the increase of COT, but at the cost of worse predictions for the conversion of some other components, such as n-butane, which is highly prominent in the naphtha feed. $COT = 835℃$ is then chosen as the temperature for performing further studies, as it is able to better balance the yields of all major components.

## 5.3 Kinetic tuning

This section focuses on extending and tuning the kinetic scheme from Joo[22] to improve the model predictions. New components and reactions were added to the original scheme. The kinetic parameters of specific reactions were manually tuned to get better match to typical yield data. The original values of kinetic parameters as reported by Joo [22] can be found in Appendix B"

The main goals of the procedure are:

- Increase ethylene production, since it is the most relevant olefin and is being under predicted;
- Decrease 1-butene, since it is being over predicted;
- Produce benzene and toluene, since these components are not being produced in any reaction;
- Crack n-nonane, which is not taking part of any reaction, exiting the furnace unreacted.

Even though the components benzene, toluene and n-nonane are present in the feed and in the Joo kinetic scheme, the authors do not include reactions involving these components, meaning they go through the cracker without reacting, which explains the reason for their composition in the feed and in the product being the same.

In order to make this components take part in the cracking reactions, it becomes necessary to add reactions from other sources that involve these components, or to "create" new reactions within the Joo scheme, considering existing reactions as a foundation. Both of these options will be explored in the next section of the work.

### 5.3.1 Addition of new components

The first change to be made is the addition of important components that are missing from the kinetic scheme. For that to happen, one must then review other kinetic schemes to add reactions to crack/produce the added component, so that it is actually part of the reaction mechanism.

The added component was acetylene ($C_2H_2$), alongside the following reactions

Table 5.8 - Added reactions for acetylene.

| Source | Added Reaction |
|---|---|
| Towfighi (reaction 103) | $C_2H_2 + H \rightarrow C_2H_3$ |
| Towfighi (reaction 142) | $C_2H_2 + H_2 \rightarrow C_2H_4$ |
| Towfighi (reaction 144) | $C_2H_2 + C_4H_6 \rightarrow C_6H_6 + H_2$ |
| Belohlav (reaction 56) | $C_2H_2 + C_2H_4 \rightarrow C_4H_6$ |
| Towfighi (reaction 74) | $C_2H_3 \rightarrow C_2H_2 + H$ |
| Towfighi (reaction 76) | $C_3H_5 \rightarrow C_2H_2 + CH_3$ |
| Belohlav (reaction 19) | $C_2H_4 \rightarrow C_2H_2 + H_2$ |

### 5.3.2 Addition of new reactions

In order to be able to be able to produce benzene and toluene and consume n-nonane, new reactions need to be added from other kinetic schemes. The schemes reviewed were the ones from Towfighi [19] and Belohlav [13], which are intended for the cracking of naphtha, being the latter a molecular scheme.

In total, two reactions were found for the production of the benzene (reaction 143 in Towfighi and reactions 9 and 35 in Belohlav) and three for the production of toluene (10 and 36 from Belohlav). These, along with the rest of the kinetic scheme, can be found in Appendix B.

These reactions are now added to the “main scheme” Joo, by modifying the FO LSKM file in order to include these five extra reactions, along with their kinetic parameters, which will be unaltered from the original source.

In the kinetic schemes considered, no reactions involving n-nonane were found. To crack this component, new reactions will have to be “created” for the scheme. The method applied is based on the fact that in the Joo scheme, the same type of reactions involving the cracking of hexane (reactions 70-82), heptane (reactions 83-99) and octane (100-119) all have the same kinetic parameters. This allows one to create the same of reaction, using n-nonane as the cracked component, and using those same kinetic parameters.

These extra reactions are also added through the Excel file of the LSKM FO.

Table 5.9 - Added reactions for the production of benzene.

| Source | Added Reaction |
|---|---|
| Towfighi (reaction 143) | $C_4H_6 + C_2H_2 \rightarrow C_6H_6 + H_2$ |
| Belohlav (reaction 9) | $C_4H_6 + C_2H_4 \rightarrow C_6H_6 + 2H_2$ |
| Belohlav (reaction 35) | $CH_3 - C_6H_5 + H_2 \rightarrow C_6H_6 + CH_4$ |

Table 5.10 - Added reactions for the production of toluene.

| Source | Added Reaction |
|---|---|
| Belohlav (reaction 10) | $C_4H_6 + C_3H_6 \rightarrow CH_3 - C_6H_5 + 2H_2$ |
| Belohlav (reaction 36) | $CH_3CH_3 - C_6H_5 + H_2 \rightarrow CH_3 - C_6H_5 + CH_4$ |

### 5.3.3 Tuning of the kinetic parameters

After adding the previously mentioned reactions into the Joo scheme, the next step is to tune the kinetic parameters of specific sets of reactions, in order to improve the prediction of the yields of the desired components.

In this work, kinetic parameter adjustment is done manually by adjusting the pre-exponential factor of certain reactions. The reactions for kinetic parameter adjustment are chosen based on the mismatch in the yields between the initial model prediction and typical results for cracking of naphtha.

Tables 5.11 and 5.12 show the reactions that had their kinetic parameters tuned, as well as the tuning factor for each considered reaction. The tuning factor represents the factor by which the pre-exponential factor is changed from the initial case (as presented in literature) to the “improved” kinetics.

Table 5.11 - Tuned reactions involving Ethylene.

| Reaction ID | Tuned Reaction | Tuning factor (×) |
|---|---|---|
| 34 | $1\_C_3H_7 \rightarrow C_2H_4 + CH_3$ | 1.25 |
| 67 | $1\_C_5H_{11} \rightarrow C_2H_4 + 1\_C_3H_7$ | 1.25 |
| 79 | $i\_C_6H_{13} \rightarrow C_2H_4 + 1\_C_4H_9$ | 1.25 |
| 95 | $1\_C_7H_{15} \rightarrow C_2H_4 + 1\_C_5H_{11}$ | 1.50 |
| 114 | $1\_C_8H_{17} \rightarrow C_2H_4 + 1\_C_6H_{13}$ | 2.00 |
| 160 | $5\_MP2 \rightarrow C_2H_4 + i\_C_4H_9$ | 1.50 |
| 191 | $6\_MH2 \rightarrow C_2H_4 + i\_C_5H_{11}$ | 1.50 |
| 228 | $7\_MHP2 \rightarrow C_2H_4 + 5\_MP2$ | 2.00 |

Table 5.12 - Tuned reactions involving 1-butene.

| Reaction ID | Tuned Reaction | Tuning factor (×) |
|---|---|---|
| 22 | $C_4H_8 \rightarrow C_3H_5 + CH_3$ | 1.50 |
| 45 | $C_4H_8 + H \rightarrow 1\_C_4H_9$ | 1.25 |
| 46 | $C_4H_8 + H \rightarrow 2\_C_4H_9$ | 1.25 |
| Belohlav - 29 | $C_4H_8 \rightarrow C_4H_6 + H_2$ | 1.50 |
| 69 | $3\_C_5H_{11} \rightarrow C_4H_8 + CH_3$ | 0.80 |
| 81 | $3\_C_6H_{13} \rightarrow C_4H_8 + 1\_C_2H_5$ | 0.65 |
| 98 | $3\_C_7H_{15} \rightarrow C_4H_8 + 1\_C_3H_7$ | 0.65 |
| 116 | $3\_C_8H_{17} \rightarrow C_4H_8 + 1\_C_4H_9$ | 0.50 |
| 189 | $4\_MH2 \rightarrow C_4H_8 + 2\_C_3H_7$ | 0.50 |
| 226 | $5\_MHP2 \rightarrow C_4H_8 + i\_C_4H_9$ | 0.50 |

## 5.3.4 Results

The simulation results using the improved kinetic scheme and its comparison to typical data is shown in table 5.13

Table 5. 13 - Simulation results for the kinetic tuning.

| Components | Feed Composition (wt. %) | | Typical data yield (%) | Simulation yield (%) | yield dev. | yield dev. (%) | | Typical data conversion (%) | Simulation conversion (%) |
|---|---|---|---|---|---|---|---|---|---|
| Hydrogen | 0 | | 0.87 | 0.53 | -0.3 | -38% | | - | - |
| Methane | 0 | | 14.36 | 11.57 | -2.8 | -19% | | - | - |
| **Ethylene** | 0 | | **27.96** | **27.99** | **0.0** | **0%** | | - | - |
| Ethane | 0 | | 3.53 | 4.74 | 1.2 | 34% | | - | - |
| **Propylene** | 0 | | **17.51** | **17.75** | **1.0** | **4%** | | - | - |
| Propane | 0 | | 0.48 | 0 | -0.5 | -100% | | - | - |
| n-butane | 6.64 | | 1.35 | 0.49 | -0.9 | -64% | | 79.6 | 81.7 |
| 1-butene | 0 | | 1.83 | 2.94 | 1.0 | 50% | | - | - |
| **1,3-butadiene** | 0 | | **5.05** | **4.85** | **-0.2** | **-5%** | | - | - |
| i-butene | 0 | | 2.91 | 1.27 | -1.7 | -58% | | - | - |
| n-pentane | 11.48 | | 1.10 | 2.82 | 1.7 | 157% | | 90.4 | 75.5 |
| i-pentane | 9.78 | | 0.97 | 1.52 | 0.6 | 58% | | 90.1 | 83.7 |
| n-hexane | 9.13 | | 0.48 | 0.92 | 0.4 | 90% | | 94.7 | 90.4 |
| i-hexane | 10.83 | | 0.43 | 1.41 | 1.0 | 218% | | 96.1 | 88.7 |
| methyl-cyclohexane | 13.32 | | 0.27 | 0.06 | -0.2 | -93% | | - | - |
| **Benzene** | **0.61** | | **5.61** | **4.74** | **-0.9** | **-18%** | | - | - |
| **Toluene** | **1.91** | | **3.67** | **3.50** | **-0.2** | **-4%** | | - | - |
| **Xylene** | **2.31** | | **2.80** | **2.05** | **-0.7** | **-27%** | | - | - |
| n-heptane | 5.31 | | 0.15 | 0 | -0.2 | -100% | | 97.1 | 100 |
| i-heptane | 7.79 | | 0.17 | 0 | -0.2 | -100% | | 97.9 | 100 |
| n-octane | 4.12 | | 0.07 | 0 | -0.1 | -100% | | - | - |
| i-octane | 6.39 | | 0.08 | 0 | -0.1 | -100% | | - | - |
| n-nonane | 6.10 | | 1.87 | 1.98 | 0.1 | 6% | | - | - |

The kinetic tuning has helped to reduce the gap between model prediction and typical data, being capable of predicting ethylene accurately, as well as the other main olefins, propylene and butadiene with deviations lower than 5%. Reasonable predictions are obtained for other key components, such as the main components present in the naphtha feed and aromatics.

# Chapter 6

# Conclusions and Future Work

In this work a furnace model with a SRT-VI coil for the stream cracking of naphtha was developed in gPROMS ProcessBuilder.

Typical operation of the naphtha cracker is simulated using two different kinetic schemes from literature. The simulation results are compared to typical yields from naphtha cracking. The kinetic scheme from Joo gave better predictions of yield, showing, however some mismatch for heavier components and aromatics.

To further improve the yield predictions, the kinetic scheme from Joo is extended by adding additional reactions. The kinetic parameters of few reactions are manually adjusted. The extended kinetic scheme with adjusted kinetic parameters gave better yield predictions.

## 6.1 Achievements

The model of a naphtha cracking furnace with SRT-VI coil is developed in gPROMS ProcessBuilder. This model together with improved kinetic schemes from literature is a useful tool for understanding the steam cracking of naphtha.

## 6.2 Future Work

The naphtha cracker model developed in the current work can be further validated using formal parameter estimation techniques. Considering additional operating data will benefit the model validation process. The reaction scheme can be further extended based on evidence in the new data.

# Bibliography


[1] H. Zimmermann and R. Walzl, “Ethylene,” in *Ullmann’s Encyclopedia of Industrial Chemistry*, Wiley-VCH Verlag GmbH & Co. KGaA, 2012.

[2] F. Sajjad, "Production of Ethylene from Naphtha - Naphtha Pracking Plant", COMSATS – Institute of Information Technology, Lahore, 2007.

[3] ICIS Chemical Business, vol. 287, nos. 4,9,10,11,15, 2015.

[4] “Petrochemical industry ethylene plant.” , Siemens, 2013, http://www.industry.usa.siemens.com/automation/us/en/process-instrumentation-and-analytics/process-analytics/pa-brochures/documents/piaap-00002-0713-ethylene.pdf, [Online; Accessed: 2016-05-12].

[5] P. Eisele and R. Killpack, “Propene,” in *Ullmann’s Encyclopedia of Industrial Chemistry*, Wiley-VCHVerlag GmbH & Co. KGaA, 2000.

[6] K. M. Sundaram, M. M. Shreehan, and E. F. Olszewski, “Ethylene,” in Kirk-Othmer Encyclopedia of Chemical Technology, John Wiley & Sons, Inc., 2000.

[7] R. Meyers, Handbook of Petrochemicals Production Processes. McGraw-Hill handbooks,McGraw-Hill Education, 2005.

[8] J. Colannino, “Ethylene furnace heat flux correlations,” Petroleum Technology Quaterly (PTQ),vol. Q1, no. 3, pp. 93–97, 2008.

[9] R. Karimzadeh, H. R. Godini, and M. Ghashghaee, “Flowsheeting of steam cracking furnaces,”Chemical Engineering Research and Design, vol. 87, no. 1, pp. 36 – 46, 2009.

[10] M. Masoumi, "Simulation, optimization and control of a thermal cracking furnace", Chemical Engineering Department, Tarbiat Modarres University,, Tehran, Iran, 2003.

[11] S. Zarinabadi, E. Ziarifar, M. S. Marouf, and A. Samimi, “Modelling and simulation for olefin production in amir kabir petrochemical,” in World Congress on Engineering and Computer Science, vol. 2, (San Francisco, USA), Oct. 2010.

[12] S. Sadrameli and A. Green, “Systematics and modeling representations of naphtha thermal cracking for olefin production,” Journal of Analytical and Applied Pyrolysis, vol. 73, no. 2, pp. 305 – 313, 2005.

[13] Z. Belohlav, P. Zamostny, and T. Herink, “The kinetic model of thermal cracking for olefins production", Chemical Engineering and Processing: Process Intensification, vol. 42, no. 6, pp. 461 – 473, 2003.

[14] K. Sundaram and G. Froment, “Modeling of thermal cracking kinetics-I: Thermal cracking of ethane, propane and their mixtures,” Chemical Engineering Science, vol. 32, no. 6, pp. 601 – 608, 1977.

[15] P. Kumar and D. Kunzru, “Modeling of naphtha pyrolysis,” Industrial & Engineering Chemistry Process Design and Development, vol. 24, no. 3, pp. 774–782, 1985.

[16] M. Dente, E. Ranzi, and A. Goossens, “Detailed prediction of olefin yields from hydrocarbon pyrolysis through a fundamental simulation model (SPYRO),” Computers & Chemical Engineering, vol. 3, 1979.

[17] K. Van Geem, M.-F. Reyniers, and G. Marin, “Challenges of modeling steam cracking of heavy feedstocks,” Oil & Gas Science and Technology - Revue de l’Institut Franc¸ais du P´ etrole, vol. 63, 2008.

[18] K. M. Sundaram and G. F. Froment, “Modelling of thermal cracking kinetics. 3. radical mechanisms for the pyrolysis of simple paraffins, olefins, and their mixtures,” Industrial & Engineering Chemistry Fundamentals, vol. 17, no. 3, pp. 174–182, 1978.

[19] J. Towfighi and R. Karimzadeh, “Development of a mechanistic model for pyrolysis of naphtha,” in Sixth Conference of the Asia-Pacific Confederation of Chemical Engineering, vol. 3, (Melbourne,Australia), Sept. 1993.

[20] E. Joo, S. Park, and M. Lee, “Pyrolysis reaction mechanism for industrial naphtha cracking furnaces”, Industrial & Engineering Chemistry Research, vol. 40, no. 11, pp. 2409–2415, 2001.

[21] T. Dijkmans, Steam cracking: from Feedstock Analysis to Plant Optimization. PhD thesis, Ghent, 2014.

[22] E. Joo, Modelling of Industrial Naphtha Thermal Cracking Furnaces. PhD thesis, Korea Advanced Institute of Science and Technology, 2000.

[23] M. Yan, “Simulation and optimization of an ethylene plant,” Master’s thesis, Texas Tech University, 2000.

[24] F. Borralho, “Detailed modelling and optimization of an ethylene plant,” Master’s thesis, Instituto Superior Técnico, 2013.

[25] J. Moreira, “Steam Cracking: Kinetics and Feed Characterisation,” Master’s thesis, Instituto Superior Técnico, November 2015.

[26] “Olefins production: Olefins by steam cracking.” , Tiszai Vegyi Kombinat (TVK), 2010, http://www.tvk.hu/repository/713326.pdf, [Online; Accessed: 2016-05-30].

[27] Ethylene spot shoots up due to lower supply in the US, http://spendmatters.com/2016/09/12/ethylene-spot-shoots-due-lower-supply-us/, [Online; Acessed 2016-10-20].

[28] “Global ethylene outlook: One product...many strategies.” , IHS, 2013, http://ihsglobalevents.com/wpc2013/files/2013/03/Carr_20131.pdf, [Online; Accessed: 2016-04-12].

[29] D. Green and R. Perry, Perry’s Chemical Engineers’ Handbook, Eighth Edition, McGraw-Hill Education, 2007.

[30] A. Chauvel and G. Lefebvre, Petrochemical Processes: 1. Synthesis-Gas Derivatives and Major Hydrocarbons. Institut Français du Pétrole Publications, Nov. 1989.

[31] M. Dente, E. Ranzi, S. Barendregt, and P. Cronin, “Steam cracking of heavy liquid feedstocks: cracking yields rigorously predicted,” in AIChe Spring National Meeting, (New Orleans, USA), 1986.

[32] K. Sundaram and G. Froment, “Modeling of thermal cracking kinetics-II: Cracking of iso-butane, of n-butane and of mixtures ethane—propane—n-butane,” Chemical Engineering Science, vol. 32, 1977.

[33] A. Karaba, P. Zamostny, Z. Belohlav, J. Lederer, and T. Herink, “Application of a semi-mechanistic model for cracking unit balance,” Chemical Engineering & Technology, vol. 38, no. 4, pp. 609–618, 2015.

[34] K. Barazandeh, O. Dehghani, M. Hamidi, E. Aryafard, and M. R. Rahimpour, “Investigation of coil outlet temperature effect on the performance of naphtha cracking furnace,” Chemical Engineering Research and Design, vol. 94, no. 0, pp. 307 – 316, 2015. Baranzadeh.

[35] J. Towfighi, H. Nazari, and R. Karimzadeh, “Simulation of light hydrocarnons pyrolysis using radical mechanism,” in Sixth Conference of the Asia-Pacific Confederation of Chemical Engineering, vol. 3, (Melbourne, Australia), Sept. 1993.

[36] M. Sedighi, K. Keyvanloo, and J. Towfighi, “Olefin production from heavy liquid hydrocarbon thermal cracking: Kinetics and product distribution,” Iranian Journal of Chemistry and Chemical Engineering, 2010.

[37] M. W. van Goethem, F. I. Kleinendorst, C. van Leeuwen, and N. van Velzen, “Equation-based SPYRO® model and solver for the simulation of the steam cracking process,” Computers & Chemical Engineering, vol. 25, no. 4–6, pp. 905 – 911, 2001.

[38] J. Towfighi, R. Karimzadeh, M. Sadrameli, A. Niaei, G. Saedi, S. Hoseini, M. Mofahrahi, and B. Mokhtarami, “SHAHAB - a pc based software for simulation of steam cracking furnaces (ethane and naphtha),” Iranian Journal of Chemical Engineering, vol. 1,2004 .

[39] R. Tewardson, “Sparse matrices,” in Mathematics in Science and Engineering, vol. 99, Academic Press Inc., 2004.

[40] T. Bergman, F. Incropera, and A. Lavine, Fundamentals of Heat and Mass Transfer, Seventh Edition, p. 544. John Wiley & Sons, Incorporated, 2011.

[41] G. Froment, K. Bischoff, and J. De Wilde, Chemical Reactor Analysis and Design, Third Edition,. p. 443. John Wiley & Sons, Incorporated, 2010.

[42] V. A. Kuritsyn et al , "Modeling of pyrolysis of straight-run naphtha in a large-capacity type SRT-VI furnace", Chemistry & Technology of Fuels & Oils, May2008.

[43] Van Geem, “From Biomass to Ethylene: Steam Cracking of Bio-Synfined Naphtha”, AIChE Spring Meeting and Global Congress on Process Safety, 2010.

[44] Patent US8163170B2 “Coil for pyrolysis heater and method of cracking”, 2012 .

[45] E. Joo, Modelling of Industrial Naphtha Thermal Cracking Furnaces. PhD thesis, Korea Advanced Institute of Science and Technology, 2000.

[46] M. Dente, E. Ranzi, “Pyrolysis of naphtha feedstocks: Automatic generation of detailed kinetics and lumping procedures,” in 20th European Symposium on Computer Aided Process Engineering, vol. 28 of Computer Aided Chemical Engineering, Elsevier, 2010.

[47] E. Ranzi, M. Dente, A. Goldaniga, G. Bozzano, and T. Faravelli, “Lumping procedures in detailed kinetic modeling of gasification, pyrolysis, partial oxidation and combustion of hydrocarbon mixtures”, Progress in Energy and Combustion Science, vol. 27,2001.

[48] “NIST chemistry webbook, NIST standard reference database number 69 (web version).” National Institute of Standards and Technology, Gaithersburg MD, 20899, http://webbook.nist.gov, [Online; Accessed: 2016-09-03].

[49] B. McBride and S.Gordon, "Coefficients for calculating thermodynamic and transport properties of individual species", NASA Technical Memorandum, 1993.

[50] The CHEMKIN Thermodynamic database, CHEMKIN Collection, Release 3.6, Reaction Design, Inc., San Diego, 2000.

[51] M. Sabbe and K. Van Geem, supportive information "First principles based simulation of ethane steam cracking", Computational Molecular Science and Engineering Forum, 2009.

[52] “Petrochemical industry ethylene plant.” , Siemens, 2013, http://www.industry.usa.siemens.com/automation/us/en/process-instrumentation-and-analytics/process-analytics/pa-brochures/documents/piaap-00002-0713-ethylene.pdf, [Online; Accessed: 2016-04-25].

[53] M. Matzopoulos, "Real-time monitoring of ethylene cracking furnaces", Advanced Process Modelling Forum 2016, London.

[54] S. Sadrameli, “Thermal/catalytic cracking of hydrocarbons for the production of olefins: A state-of-the-art review i: Thermal cracking review,” Fuel, vol. 140, no. 0, pp. 102 – 115, 2015.

# Appendix A

# Thermodynamics

The following two tables contain a comparison of physical properties (for both molecular and radical components) between various sources, from Multiflash (main physical property package used in the current work) and others, found in literature (48) (49) (50)

Table A.1 – Comparison of physical properties of molecular species between Multiflash and other databanks.

| SPECIES | M.W. (g/mol) | $\Delta_f H°$(kJ/mol) | | | | $C_p^{1100K}$(J/mol/K) | | | |
|---|---|---|---|---|---|---|---|---|---|
| | | NIST | CHEMKIN | Gordon&McBride | Multiflash | NIST | CHEMKIN | Gordon&McBride | Multiflash |
| Molecules | | | | | | | | | |
| Water | 18,02 | -241,83 | -241,84 | -241,82 | -241,81 | 42,52 | 42,64 | 42,66 | 42,55 |
| Hydrogen | 2,02 | 0,00 | 0,00 | 0,00 | 0,00 | 30,58 | 30,63 | 30,65 | 30,61 |
| Methane | 16,04 | -74.87 to -73.40 | -74,89 | -74,60 | -74,52 | 77,92 | 75,60 | 77,47 | 76,83 |
| Acetylene | 26,04 | 226.73 to 227.40 | 226,73 | 228,20 | 228,2 | 69,91 | 70,19 | 69,79 | 69,03 |
| Ethylene | 28,05 | 52,47 | 52,47 | 52,50 | 52,51 | 98,00 | 97,97 | 97,82 | 98,84 |
| Ethane | 30,07 | -84.67 to -83.80 | -83,68 | -83,85 | -83,82 | 128,55 | 127,86 | 128,11 | 128,69 |
| Propadiene | 40,06 | - | 199,45 | 190,92 | 190,50 | 121,40 | 123,32 | 121,05 | 121,42 |
| Propylene | 42,08 | 20,41 | 20,42 | 19,71 | 20,23 | 150,83 | 150,05 | 150,33 | 151,48 |
| Propane | 44,10 | -104.7 to -103.8 | -103,76 | -104,68 | -104,68 | 182,67 | 181,69 | 182,97 | 182,74 |
| 1,3-Butadiene | 54,09 | 108.8 to 111.9 | 118,53 | 110,00 | 109,24 | 179,36 | 178,04 | 178,17 | 179,70 |
| 1-Butene | 56,11 | -0,63 | -0,54 | -0,54 | -0,50 | 204,55 | 204,98 | 204,00 | 205,07 |
| 2-Butene | 56,11 | -10.8 to -7.70 | - | -7,40 | -7,40 | 203,06 | - | 201,61 | 202,27 |
| i-Butene | 56,11 | -17,90 | - | -17,10 | -17,10 | 204,03 | - | 203,38 | 204,30 |
| n-Butane | 58,12 | -127.1 to -125.6 | -128,20 | -125,79 | -125,79 | 237,48 | 242,63 | 236,81 | 237,57 |
| i-Butane | 58,12 | -135.6 to -134.2 | -133,97 | -134,99 | -134,99 | 238,49 | 239,64 | 237,71 | 238,56 |
| 1-Buten-3-yne, 2-methyl- | 66,10 | 259,00 | - | 0,00 | 260,00 | - | - | 0,00 | 197,40 |
| 2-methyl-1,3-butadiene (Isoprene) | 68,12 | 75,70 | - | 0,00 | 75,73 | 222,50 | - | 0,00 | 231,73 |
| 2-methyl-2-butene | 70,13 | -41,50 | - | 0,00 | -41,80 | 255,89 | - | 0,00 | 256,08 |
| Cyclopentadiene | 66,10 | 136,20 | 133,89 | 134,30 | 130,80 | 199,04 | 195,44 | 198,50 | 199,17 |
| 1-pentene-3-yne | 66,10 | - | - | 0,00 | 249,00 | - | - | 0,00 | 194,46 |
| 1-pentene-4-yne | 66,10 | - | - | 0,00 | 269,00 | - | - | 0,00 | 194,72 |
| Cyclopentene | 68,12 | 32.60 to 36.0 | - | 33,90 | 32,30 | 229,60 | - | 228,88 | 229,93 |
| 1,3-Pentadiene | 68,12 | 75.77 to 82.72 | - | 0,00 | 82,78 | 229,60 | - | 0,00 | 229,77 |
| 1,4-Pentadiene | 68,12 | 106,30 | - | 0,00 | 106,38 | 233,40 | - | 0,00 | 233,56 |
| 1-Pentene | 70,13 | -22,00 | - | -21,28 | -21,62 | 256,40 | - | 255,58 | 259,03 |
| Cyclopentane | 70,13 | -77.24 to -76.4 | - | -78,40 | -77,03 | 260,76 | - | 259,84 | 261,46 |
| n-Pentane | 72,15 | -147.1 to -146.4 | -146,44 | -146,76 | -146,76 | 293,72 | 292,00 | 294,11 | 294,35 |
| i-Pentane | 72,15 | -154.5 to -153.7 | - | -153,70 | -153,70 | 299,57 | - | 298,02 | 300,40 |
| Cyclopentene-4-methyl | 82,15 | 15,00 | - | 0,00 | 13,54 | - | - | 0,00 | 282,005 |
| Methylcyclopentane | 84,16 | -108.1 to -106.0 | - | 0,00 | -106,2 | 317,1 | - | 0,00 | 317,308 |
| Benzene | 78,11 | 79.90 to 82.93 | 82,89 | 82,88 | 82,88 | 219,56 | 220,70 | 210,43 | 219,71 |
| 1,4-Hexadiene | 82,15 | 74.0 to 77.0 | - | 0,00 | 71,87 | - | - | 0,00 | 278,618 |
| Cyclohexene | 82,15 | -7.10 to -4.32 | -4,18 | -4,60 | -4,6 | 287,83 | 288,74 | 336,34 | 288,30 |
| Cyclohexane | 84,16 | -124.6 to -123.1 | - | -123,30 | -123,3 | 328,66 | - | 327,04 | 329,785 |
| n-Hexane | 86,18 | -167,2 | -166,94 | 0,00 | -166,94 | 345,18 | 341,72 | 0,00 | 345,91 |
| i-Hexane | 86,18 | -174,3 | - | 0,00 | -174,55 | 351,87 | - | 0,00 | 353,147 |
| Toluene | 92,14 | 48.00 to 50.10 | 49,40 | 50,17 | 50,17 | 271,80 | 271,96 | 270,55 | 272,37 |
| Styrene | 104,15 | 131.5 to 151.5 | - | 148,30 | 147,4 | 295,80 | - | 294,78 | 295,064 |
| Ethylbenzene | 106,17 | 29.8 to 48 | - | 29,92 | 29,92 | 326,56 | - | 325,57 | 327,058 |
| o-Xylene | 106,17 | 19,0 | - | 0,00 | 19,08 | 324,90 | - | 0,00 | 325,24 |
| m-Xylene | 106,17 | 17,2 | - | 0,00 | 17,32 | 324,10 | - | 0,00 | 324,71 |
| p-Xylene | 106,17 | 17,9 | - | 0,00 | 18,03 | 324,20 | - | 0,00 | 324,76 |
| 1,2,4-trimethylbenzene | 120,19 | -13,9 | - | 0,00 | -13,8 | 377,30 | - | 0,00 | 377,592 |
| 1,2,4,5-tetramethylbenzene (durene) | 134,22 | -47.1 to -45.3 | - | 0,00 | -47,1 | 430,80 | - | 0,00 | 431,726 |
| n-Heptane | 100,20 | -189.3 to -187.9 | - | 276,21 | -187,65 | 397,06 | - | 396,41 | 398,10 |
| i-Heptane | 100,20 | -196.2 to -195.0 | - | 0,00 | -194,6 | 403,34 | - | 0,00 | 404,53 |
| Cyclooctene | 110,20 | -22,7 | - | 0,00 | -32,24 | - | - | 0,00 | 403,519 |
| Cyclooctane | 112,21 | -121,6 | - | 0,00 | -125,8 | 432,79 | - | 0,00 | 433,21 |
| n-Octane | 114,23 | -208,6 | - | 314,12 | -208,75 | 448,52 | - | 447,33 | 449,69 |
| i-Octane | 114,23 | -215,5 | - | -224,01 | -215,35 | 454,80 | - | 474,68 | 456,411 |
| n-Nonane | 128,257 | -228,3 | - | 0,00 | -228,74 | 499,99 | - | 0,00 | 501,447 |
| i-Nonane | 128,257 | - | - | 0,00 | -234,8 | - | - | 0,00 | 507,004 |

Table A.2 - Comparison of physical properties of radical species between Multiflash and other databanks.

| Radicals | | | | | | | | | |
|---|---|---|---|---|---|---|---|---|---|
| H· | 1,01 | 218,00 | 217,99 | 218,00 | - | 20,81 | 20,79 | 20,79 | - |
| CH3· | 15,03 | 145,69 | 145,69 | 146,90 | - | 61,171 | 61,24 | 61,08 | - |
| C2H3· | 27,05 | 299,0 | 286,19 | 299,74 | - | - | 80,78 | 82,48 | - |
| C2H5· | 29,06 | 119,00 | 117,15 | 118,66 | - | - | 110,49 | 115,04 | - |
| C3H5· | 41,07 | 171,00 | 161,92 | 169,00 | - | - | 141,99 | 136,08 | - |
| nC3H7· | 43,09 | 100,00 | 94,56 | 100,50 | - | - | 166,21 | 165,95 | - |
| iC3H7· | 43,09 | 90,00 | 77,82 | 93,30 | - | - | 166,71 | 163,12 | - |
| 1C4H9· | 57,1151 | - | - | 66,53 | - | - | - | 220,34 | - |
| 2C4H9· | 57,1151 | 69,00 | - | 71,00 | - | - | - | 217,11 | - |
| iC4H9· | 57,1151 | 70,00 | - | 57,32 | - | - | - | 221,23 | - |
| cC5H9· | 69,1261 | - | - | 0,00 | - | - | - | 0,00 | - |
| 1C5H11· | 71,1419 | - | - | 45,81 | - | - | - | 274,28 | - |
| 2C5H11· | 71,1419 | - | - | 0,00 | - | - | - | 0,00 | - |
| iC5H11· | 71,1419 | - | - | 0,00 | - | - | - | 0,00 | - |
| cC6H11· | 83,1529 | - | - | 0,00 | - | - | - | 0,00 | - |
| 1C6H13· | 85,1687 | - | - | 240,98 | - | - | - | 328,13 | - |
| 2C6H13· | 85,1687 | - | - | 0,00 | - | - | - | 0,00 | - |
| iC6H13· | 85,1687 | - | - | 0,00 | - | - | - | 0,00 | - |

# Appendix B

# Kinetics

Tables B.1 to B.4 show the kinetic mechanism of Joo (45), containing all the reactions that are part of the scheme and the kinetic parameters for each reaction: Activation Energy, $E_a$, in $J/mol$ and Pre-Exponential Factor, $k_0$, in $s^{-1}$ for first order reactions and $m^3\ mol^{-1}\ s^{-1}$ for second order reactions.

Table B.1 - Reaction mechanism proposed by Joo: reactions 1-48.

| | Reactions considered | $k_0$ | $E_a\ (J/mol)$ |
|---|---|---|---|
| 1 | iC4H10=>CH3+C3H7_2 | 5.01E+17 | 352309.4 |
| 2 | nC5H12=>CH3+C4H9_1 | 6.16E+17 | 357748.9 |
| 3 | nC5H12=>C2H5+C3H7_1 | 1.26E+17 | 341430.5 |
| 4 | iC5H12=>CH3+C4H9_2 | 3.16E+17 | 351472.6 |
| 5 | iC5H12=>C2H5+C3H7_2 | 7.94E+16 | 335154.2 |
| 6 | iC5H12=>CH3+iC4H9 | 2.51E+17 | 357330.5 |
| 7 | C6H14=>C2H5+C4H9_1 | 6.31E+16 | 342685.8 |
| 8 | C6H14=>2C3H7_1 | 3.16E+16 | 342685.8 |
| 9 | MP2=>CH3+C5H11_2 | 1.26E+17 | 346870 |
| 10 | MP2=>C3H7_1+C3H7_2 | 3.98E+16 | 331388.4 |
| 11 | MP2=>iC4H9+C2H5 | 6.31E+16 | 338920 |
| 12 | C6H12_1=>C3H7_1+aC3H5 | 2.51E+16 | 297496.4 |
| 13 | C7H16=>CH3+C6H13_1 | 2.00E+16 | 300007 |
| 14 | C7H16=>C2H5+C5H11_1 | 2.00E+16 | 280006.5 |
| 15 | C8H18=>C3H7_1+C5H11_1 | 4.00E+16 | 220005.1 |
| 16 | MH2=>CH3+C6H13_2 | 4.00E+16 | 300007 |
| 17 | MHP2=>CH3+C7H15_2 | 4.00E+16 | 300007 |
| 18 | MC5=>CH3+cC5H9 | 1.00E+16 | 300007 |
| 19 | MC6=>CH3+cC6H11 | 1.00E+16 | 300007 |
| 20 | C2H4+CH3=>C2H3+CH4 | 6.31E+12 | 62763 |
| 21 | 2C2H3=>BDE13 | 1.26E+13 | 41842 |
| 22 | C4H8_1=>CH3+aC3H5 | 6.31E+15 | 306701.7 |
| 23 | H+C2H6=>H2+C2H5 | 5.01E+14 | 33473.6 |
| 24 | H+C4H10=>H2+C4H9_1 | 6.31E+14 | 33473.6 |
| 25 | H+C4H10=>H2+C4H9_2 | 6.31E+14 | 33473.6 |
| 26 | CH3+H2=>CH4+H | 1.59E+12 | 49791.9 |
| 27 | CH3+C2H6=>CH4+C2H5 | 1.00E+13 | 49791.9 |
| 28 | CH3+C4H10=>CH4+C4H9_1 | 1.00E+13 | 49791.9 |
| 29 | CH3+C4H10=>CH4+C4H9_2 | 6.31E+12 | 49791.9 |
| 30 | C2H5+H2=>C2H6+H | 1.26E+12 | 58578.8 |
| 31 | C2H5+C2H4=>C3H6+CH3 | 3.16E+12 | 79499.8 |
| 32 | C2H5+C3H6=>C2H6+aC3H5 | 3.98E+12 | 58578.8 |
| 33 | C2H5=>C2H4+H | 7.94E+13 | 191208 |
| 34 | C3H7_1=>C2H4+CH3 | 5.01E+13 | 142262.7 |
| 35 | C3H7_1=>C3H6+H | 2.00E+14 | 163183.7 |
| 36 | C3H7_2=>C3H6+H | 2.00E+14 | 179920.5 |
| 37 | C4H9_1=>C4H8_1+H | 1.26E+14 | 163183.7 |
| 38 | C4H9_1=>C2H4+C2H5 | 1.59E+14 | 129710.1 |
| 39 | C4H9_2=>C4H8_2+H | 1.00E+14 | 171552.1 |
| 40 | C4H9_2=>C3H6+CH3 | 2.00E+14 | 142262.7 |
| 41 | iC4H9=>C3H6+CH3 | 3.00E+14 | 142262.7 |
| 42 | H+C2H4=>C2H5 | 1.00E+14 | 8368.4 |
| 43 | H+C3H6=>C3H7_1 | 3.98E+13 | 8368.4 |
| 44 | H+C3H6=>C3H7_2 | 3.98E+13 | 8368.4 |
| 45 | H+C4H8_1=>C4H9_1 | 2.51E+13 | 8368.4 |
| 46 | H+C4H8_1=>C4H9_2 | 7.94E+13 | 8368.4 |
| 47 | H+C4H8_2=>C4H9_2 | 1.00E+14 | 10460.5 |
| 48 | H+iC4H8=>iC4H9 | 1.00E+14 | 8368.4 |

Table B.2 - Reaction mechanism proposed by Joo: reactions 49-120.

| | | | |
|---|---|---|---|
| 49 | CH3+H=>CH4 | 2.00E+14 | 0 |
| 50 | 2CH3=>C2H6 | 2.00E+13 | 0 |
| 51 | CH3+C2H5=>C3H8 | 1.00E+13 | 0 |
| 52 | CH3+aC3H5=>C4H8_1 | 7.94E+12 | 0 |
| 53 | 2C2H5=>C4H10 | 2.00E+12 | 0 |
| 54 | C2H6=>C2H4+H2 | 7.94E+13 | 297078 |
| 55 | C3H8=>C3H6+H2 | 7.94E+11 | 158999.5 |
| 56 | C3H7_2=>C3H7_1 | 1.00E+14 | 158999.5 |
| 57 | CH3+nC5H12=>CH4+C5H11_1 | 2.00E+11 | 56486.7 |
| 58 | CH3+nC5H12=>CH4+C5H11_2 | 2.00E+11 | 46863 |
| 59 | CH3+nC5H12=>CH4+C5H11_3 | 1.00E+11 | 46863 |
| 60 | C2H5+nC5H12=>C2H6+C5H11_1 | 2.00E+11 | 56486.7 |
| 61 | C2H5+nC5H12=>C2H6+C5H11_2 | 2.00E+11 | 46863 |
| 62 | C2H5+nC5H12=>C2H6+C5H11_3 | 1.00E+11 | 46863 |
| 63 | C3H7_1+nC5H12=>C3H8+C5H11_2 | 2.00E+11 | 46863 |
| 64 | C3H7_2+nC5H12=>C3H8+C5H11_2 | 2.00E+11 | 51047.2 |
| 65 | C5H11_1=>C5H11_2 | 2.00E+11 | 76570.8 |
| 66 | C5H11_2=>C5H11_1 | 3.00E+11 | 90378.7 |
| 67 | C5H11_1=>C2H4+C3H7_1 | 1.00E+14 | 125525.9 |
| 68 | C5H11_2=>C3H6+C2H5 | 1.00E+14 | 129710.1 |
| 69 | C5H11_3=>C4H8_1+CH3 | 1.00E+14 | 138078.5 |
| 70 | CH3+C6H14=>CH4+C6H13_2 | 2.00E+11 | 46863 |
| 71 | CH3+C6H14=>CH4+C6H13_3 | 2.00E+11 | 46863 |
| 72 | C2H5+C6H14=>C2H6+C6H13_1 | 2.00E+11 | 56486.7 |
| 73 | C2H5+C6H14=>C2H6+C6H13_2 | 2.00E+11 | 46863 |
| 74 | C2H5+C6H14=>C2H6+C6H13_3 | 2.00E+11 | 46863 |
| 75 | C6H13_1=>C6H13_2 | 3.17E+10 | 51047.2 |
| 76 | C6H13_2=>C6H13_1 | 4.76E+10 | 64855.1 |
| 77 | C6H13_1=>C6H13_3 | 2.00E+11 | 76570.8 |
| 78 | C6H13_3=>C6H13_1 | 3.00E+11 | 90378.7 |
| 79 | C6H13_1=>C2H4+C4H9_1 | 1.00E+14 | 125525.9 |
| 80 | C6H13_2=>C3H6+C3H7_1 | 1.00E+14 | 129710.1 |
| 81 | C6H13_3=>C4H8_1+C2H5 | 1.00E+14 | 129710.1 |
| 82 | C6H13_3=>C5H10_2+CH3 | 1.00E+14 | 138078.5 |
| 83 | CH3+C7H16=>CH4+C7H15_3 | 2.00E+11 | 46863 |
| 84 | CH3+C7H16=>CH4+C7H15_4 | 1.00E+11 | 46863 |
| 85 | C2H5+C7H16=>C2H6+C7H15_1 | 2.00E+11 | 56486.7 |
| 86 | C2H5+C7H16=>C2H6+C7H15_2 | 2.00E+11 | 46863 |
| 87 | C2H5+C7H16=>C2H6+C7H15_3 | 2.00E+11 | 46863 |
| 88 | C2H5+C7H16=>C2H6+C7H15_4 | 1.00E+11 | 46863 |
| 89 | C7H15_1=>C7H15_3 | 3.17E+10 | 51047.2 |
| 90 | C7H15_3=>C7H15_1 | 4.76E+10 | 64855.1 |
| 91 | C7H15_1=>C7H15_4 | 2.00E+11 | 76570.8 |
| 92 | C7H15_4=>C7H15_1 | 3.00E+11 | 90378.7 |
| 93 | C7H15_2=>C7H15_3 | 2.00E+11 | 80755 |
| 94 | C7H15_3=>C7H15_2 | 2.00E+11 | 80755 |
| 95 | C7H15_1=>C2H4+C5H11_1 | 1.00E+14 | 125525.9 |
| 96 | C7H15_2=>C3H6+C4H9_1 | 1.00E+14 | 129710.1 |
| 97 | C7H15_3=>C6H12_1+CH3 | 1.00E+14 | 138078.5 |
| 98 | C7H15_3=>C4H8_1+C3H7_1 | 1.00E+14 | 129710.1 |
| 99 | C7H15_4=>C5H10_1+C2H5 | 1.00E+14 | 129710.1 |
| 100 | CH3+C8H18=>CH4+C8H17_1 | 2.00E+11 | 56486.7 |
| 101 | CH3+C8H18=>CH4+C8H17_2 | 2.00E+11 | 46863 |
| 102 | CH3+C8H18=>CH4+C8H17_3 | 2.00E+11 | 46863 |
| 103 | CH3+C8H18=>CH4+C8H17_4 | 2.00E+11 | 46863 |
| 104 | C2H5+C8H18=>C2H6+C8H17_1 | 2.00E+11 | 56486.7 |
| 105 | C2H5+C8H18=>C2H6+C8H17_2 | 2.00E+11 | 46863 |
| 106 | C2H5+C8H18=>C2H6+C8H17_3 | 2.00E+11 | 46863 |
| 107 | C2H5+C8H18=>C2H6+C8H17_4 | 2.00E+11 | 46863 |
| 108 | C8H17_1=>C8H17_4 | 2.00E+11 | 76570.8 |
| 109 | C8H17_4=>C8H17_1 | 3.00E+11 | 90378.7 |
| 110 | C8H17_2=>C8H17_4 | 2.00E+11 | 80755 |
| 111 | C8H17_4=>C8H17_2 | 2.00E+11 | 80755 |
| 112 | C8H17_2=>C8H17_3 | 3.17E+10 | 55231.4 |
| 113 | C8H17_3=>C8H17_2 | 3.17E+10 | 55231.4 |
| 114 | C8H17_1=>C2H4+C6H13_1 | 1.00E+14 | 125525.9 |
| 115 | C8H17_2=>C3H6+C5H11_1 | 1.00E+14 | 129710.1 |
| 116 | C8H17_3=>C4H8_1+C4H9_1 | 1.00E+14 | 129710.1 |
| 117 | C8H17_3=>C7H14_1+CH3 | 1.00E+14 | 138078.5 |
| 118 | C8H17_4=>C5H10_1+C3H7_1 | 1.00E+14 | 129710.1 |
| 119 | C8H17_4=>C6H12_1+C2H5 | 1.00E+14 | 129710.1 |
| 120 | CH3+iC5H12=>CH4+iC5H11_1 | 1.00E+11 | 56486.7 |

Table B.3 - Reaction mechanism proposed by Joo: reactions 121-195.

| | | | |
|---|---|---|---|
| 121 | CH3+iC5H12=>CH4+iC5H11_2 | 1.00E+11 | 37657.8 |
| 122 | CH3+iC5H12=>CH4+iC5H11_3 | 1.00E+11 | 46863 |
| 123 | CH3+iC5H12=>CH4+iC5H11_4 | 1.00E+11 | 56486.7 |
| 124 | C2H5+iC5H12=>C2H6+iC5H11_1 | 1.00E+11 | 56486.7 |
| 125 | C2H5+iC5H12=>C2H6+iC5H11_2 | 1.00E+11 | 37657.8 |
| 126 | C2H5+iC5H12=>C2H6+iC5H11_3 | 1.00E+11 | 46863 |
| 127 | C2H5+iC5H12=>C2H6+iC5H11_4 | 1.00E+11 | 56486.7 |
| 128 | C3H7_1+iC5H12=>C3H8+iC5H11_2 | 1.00E+11 | 37657.8 |
| 129 | C3H7_2+iC5H12=>C3H8+iC5H11_2 | 1.00E+11 | 41842 |
| 130 | iC5H11_1=>iC5H11_4 | 3.00E+11 | 86194.5 |
| 131 | iC5H11_4=>iC5H11_1 | 6.00E+11 | 86194.5 |
| 132 | iC5H11_1=>C3H6+C2H5 | 1.00E+14 | 125525.9 |
| 133 | iC5H11_1=>C4H8_1+CH3 | 1.00E+14 | 133894.3 |
| 134 | iC5H11_2=>iC4H8+CH3 | 1.00E+14 | 140170.6 |
| 135 | iC5H11_3=>C4H8_2+CH3 | 2.00E+14 | 138078.5 |
| 136 | iC5H11_4=>C2H4+C3H7_2 | 1.00E+14 | 117157.5 |
| 137 | CH3+MP2=>CH4+MP2_2 | 1.00E+11 | 37657.8 |
| 138 | CH3+MP2=>CH4+MP2_5 | 1.00E+11 | 56486.7 |
| 139 | CH3+MP2=>CH4+MP2_1 | 1.00E+11 | 56486.7 |
| 140 | CH3+MP2=>CH4+MP2_4 | 1.00E+11 | 46863 |
| 141 | CH3+MP2=>CH4+MP2_3 | 1.00E+11 | 46863 |
| 142 | C2H5+MP2=>C2H6+MP2_2 | 1.00E+11 | 37657.8 |
| 143 | C2H5+MP2=>C2H6+MP2_5 | 1.00E+11 | 56486.7 |
| 144 | C2H5+MP2=>C2H6+MP2_1 | 1.00E+11 | 56486.7 |
| 145 | C2H5+MP2=>C2H6+MP2_4 | 1.00E+11 | 46863 |
| 146 | C2H5+MP2=>C2H6+MP2_3 | 1.00E+11 | 46863 |
| 147 | C3H7_2+MP2=>C3H8+MP2_2 | 1.00E+11 | 41842 |
| 148 | MP2_1=>MP2_4 | 2.00E+11 | 76570.8 |
| 149 | MP2_4=>MP2_1 | 6.00E+11 | 90378.7 |
| 150 | MP2_1=>MP2_5 | 4.76E+10 | 60670.9 |
| 151 | MP2_5=>MP2_1 | 9.51E+10 | 60670.9 |
| 152 | MP2_2=>MP2_5 | 3.00E+11 | 92470.8 |
| 153 | MP2_5=>MP2_2 | 1.00E+11 | 67365.6 |
| 154 | MP2_1=>C3H6+C3H7_1 | 1.00E+14 | 125525.9 |
| 155 | MP2_1=>C5H10_1+CH3 | 1.00E+14 | 133894.3 |
| 156 | MP2_2=>iC4H8+C2H5 | 1.00E+14 | 131802.2 |
| 157 | MP2_3=>M3BE1+CH3 | 1.00E+14 | 138078.5 |
| 158 | MP2_3=>C5H10_2+CH3 | 2.00E+14 | 138078.5 |
| 159 | MP2_4=>C3H6+C3H7_2 | 1.00E+14 | 121341.7 |
| 160 | MP2_5=>C2H4+iC4H9 | 1.00E+14 | 125525.9 |
| 161 | CH3+MH2=>CH4+MH2_1 | 1.00E+11 | 56486.7 |
| 162 | CH3+MH2=>CH4+MH2_2 | 1.00E+11 | 37657.8 |
| 163 | CH3+MH2=>CH4+MH2_3 | 1.00E+11 | 46863 |
| 164 | CH3+MH2=>CH4+MH2_4 | 1.00E+11 | 46863 |
| 165 | CH3+MH2=>CH4+MH2_5 | 1.00E+11 | 46863 |
| 166 | CH3+MH2=>CH4+MH2_6 | 1.00E+11 | 56486.7 |
| 167 | C2H5+MH2=>C2H6+MH2_1 | 1.00E+11 | 56486.7 |
| 168 | C2H5+MH2=>C2H6+MH2_2 | 1.00E+11 | 37657.8 |
| 169 | C2H5+MH2=>C2H6+MH2_3 | 1.00E+11 | 46863 |
| 170 | C2H5+MH2=>C2H6+MH2_4 | 1.00E+11 | 46863 |
| 171 | C2H5+MH2=>C2H6+MH2_5 | 1.00E+11 | 46863 |
| 172 | C2H5+MH2=>C2H6+MH2_6 | 1.00E+11 | 56486.7 |
| 173 | MH2_1=>MH2_4 | 2.00E+11 | 76570.8 |
| 174 | MH2_4=>MH2_1 | 6.00E+11 | 90378.7 |
| 175 | MH2_1=>MH2_5 | 3.17E+10 | 51047.2 |
| 176 | MH2_5=>MH2_1 | 9.51E+10 | 64855.1 |
| 177 | MH2_2=>MH2_5 | 2.00E+11 | 82847.1 |
| 178 | MH2_5=>MH2_2 | 1.00E+11 | 71549.8 |
| 179 | MH2_2=>MH2_6 | 4.76E+10 | 66947.2 |
| 180 | MH2_6=>MH2_2 | 1.59E+10 | 41842 |
| 181 | MH2_3=>MH2_6 | 3.00E+11 | 90378.7 |
| 182 | MH2_6=>MH2_3 | 2.00E+11 | 76570.8 |
| 183 | MH2_1=>C6H12_1+CH3 | 1.00E+14 | 133894.3 |
| 184 | MH2_1=>C3H6+C4H9_1 | 1.00E+14 | 125525.9 |
| 185 | MH2_2=>iC4H8+C3H7_1 | 1.00E+14 | 131802.2 |
| 186 | MH2_3=>M3BE1+C2H5 | 1.00E+14 | 129710.1 |
| 187 | MH2_3=>C6H12_2+CH3 | 2.00E+14 | 138078.5 |
| 188 | MH2_4=>M4PE1+CH3 | 1.00E+14 | 138078.5 |
| 189 | MH2_4=>C4H8_1+C3H7_2 | 1.00E+14 | 121341.7 |
| 190 | MH2_5=>C3H6+iC4H9 | 1.00E+14 | 129710.1 |
| 191 | MH2_6=>C2H4+iC5H11_4 | 1.00E+14 | 125525.9 |
| 192 | CH3+MHP2=>CH4+MHP2_1 | 1.00E+11 | 56486.7 |
| 193 | CH3+MHP2=>CH4+MHP2_2 | 1.00E+11 | 37657.8 |
| 194 | CH3+MHP2=>CH4+MHP2_3 | 1.00E+11 | 46863 |
| 195 | CH3+MHP2=>CH4+MHP2_4 | 1.00E+11 | 46863 |

Table B.4 - Reaction mechanism proposed by Joo: reactions 196-231.

| | | | |
|---|---|---|---|
| 196 | CH3+MHP2=>CH4+MHP2_5 | 1.00E+11 | 46863 |
| 197 | CH3+MHP2=>CH4+MHP2_6 | 1.00E+11 | 46863 |
| 198 | CH3+MHP2=>CH4+MHP2_7 | 1.00E+11 | 56486.7 |
| 199 | C2H5+MHP2=>C2H6+MHP2_1 | 1.00E+11 | 56486.7 |
| 200 | C2H5+MHP2=>C2H6+MHP2_2 | 1.00E+11 | 37657.8 |
| 201 | C2H5+MHP2=>C2H6+MHP2_3 | 1.00E+11 | 46863 |
| 202 | C2H5+MHP2=>C2H6+MHP2_4 | 1.00E+11 | 46863 |
| 203 | C2H5+MHP2=>C2H6+MHP2_5 | 1.00E+11 | 46863 |
| 204 | C2H5+MHP2=>C2H6+MHP2_6 | 1.00E+11 | 46863 |
| 205 | C2H5+MHP2=>C2H6+MHP2_7 | 1.00E+11 | 56486.7 |
| 206 | MHP2_1=>MHP2_4 | 2.00E+11 | 76570.8 |
| 207 | MHP2_4=>MHP2_1 | 6.00E+11 | 90378.7 |
| 208 | MHP2_1=>MHP2_5 | 3.17E+10 | 51047.2 |
| 209 | MHP2_5=>MHP2_1 | 9.51E+10 | 64855.1 |
| 210 | MHP2_2=>MHP2_5 | 2.00E+11 | 82847.1 |
| 211 | MHP2_5=>MHP2_2 | 1.00E+11 | 71549.8 |
| 212 | MHP2_2=>MHP2_6 | 3.17E+10 | 57323.5 |
| 213 | MHP2_6=>MHP2_2 | 1.59E+10 | 46026.2 |
| 214 | MHP2_3=>MHP2_6 | 2.00E+11 | 80755 |
| 215 | MHP2_6=>MHP2_3 | 2.00E+11 | 80755 |
| 216 | MHP2_3=>MHP2_7 | 4.76E+10 | 64855.1 |
| 217 | MHP2_7=>MHP2_3 | 3.17E+10 | 51047.2 |
| 218 | MHP2_1=>C3H6+C5H11_1 | 1.00E+14 | 125525.9 |
| 219 | MHP2_1=>C7H14_1+CH3 | 1.00E+14 | 133894.3 |
| 220 | MHP2_2=>iC4H8+C4H9_1 | 1.00E+14 | 131802.2 |
| 221 | MHP2_3=>C7H14_2+CH3 | 2.00E+14 | 138078.5 |
| 222 | MHP2_3=>M3BE1+C3H7_1 | 1.00E+14 | 129710.1 |
| 223 | MHP2_4=>M4PE1+C2H5 | 1.00E+14 | 129710.1 |
| 224 | MHP2_4=>C5H10_1+C3H7_2 | 1.00E+14 | 121341.7 |
| 225 | MHP2_5=>M2HE5+CH3 | 1.00E+14 | 138078.5 |
| 226 | MHP2_5=>C4H8_1+iC4H9 | 1.00E+14 | 129710.1 |
| 227 | MHP2_6=>C3H6+iC5H11_4 | 1.00E+14 | 129710.1 |
| 228 | MHP2_7=>C2H4+MP2_5 | 1.00E+14 | 125525.9 |
| 229 | cC5H9=>C2H4+aC3H5 | 1.00E+13 | 81435.9 |
| 230 | cC6H11=>BDE13+C2H5 | 1.00E+13 | 111256.6 |
| 231 | cC6H11=>C3H6+aC3H5 | 1.00E+13 | 86056 |

Table B.5 compares the kinetic parameters from the same reactions taken from different published kinetic mechanisms (the ones that were mainly used in the current work – Joo (22) and Towfighi (19)) and other sources (online databank NIST (48) and work published by Sabbe and Van Geem (51)). This comparison is of high importance since kinetic tuning was implemented in this work, in which reactions from different sources were added together. For this “unification” to be successful and reliable, one must guarantee that the kinetic parameters are in agreement when taken from different sources.

Table B.5 - Comparison of kinetic parameters between several published kinetic mechanisms and other data sources.

| | log 10 Pre-exponential factor | | | | | Activation energy (kJ/mol) | | | | |
|---|---|---|---|---|---|---|---|---|---|---|
| Reference: | NIST | Sundaram andFroment | Towfighi | Joo | Sabbe/Van Geem | NIST (a) | Sundaram [17] (b) | Towfighi [18] (c) | Joo [26] (d) | Sabbe/Van Geem |
| 1-$C_3H_7$· → $C_2H_4$ + $CH_3$· | 12-13 | 13,60 | 13,60 | 13,70 | - | ≈130 | 136,40 | 136,40 | 142,30 | - |
| 1-$C_3H_7$· → $C_3H_6$ + H· | 13 | 13,30 | 13,30 | 14,30 | - | ≈150 | 160,67 | 160,67 | 163,20 | - |
| 2-$C_3H_7$· → $C_3H_6$ + H· | 13 | 13,30 | 13,30 | 14,30 | - | ≈160 | 161,92 | 161,92 | 179,90 | - |
| 1-$C_4H_8$ → $C_3H_5$· + $CH_3$· | 16 | 16,90 | 16,90 | 15,80 | - | 305 | 309,62 | 309,62 | 306,70 | - |
| 1-$C_4H_9$· → 1-$C_4H_8$ + H· | 13-14 | 12,20 | 12,20 | 14,10 | - | ≈155 | 117,15 | 117,15 | 163,20 | - |
| 1-$C_4H_9$· → $C_2H_5$· + $C_2H_4$ | 13-14 | 13,00 | 13,00 | 14,20 | - | ≈120 | 153,13 | 153,13 | 129,70 | - |
| 2-$C_4H_9$· → $C_2H_5$· + $C_2H_4$ | - | 13,40 | 13,40 | 14,30 | - | 123 | 133,47 | 133,47 | 142,20 | - |
| i-$C_4H_9$· → $C_3H_6$ + $CH_3$· | 12-13 | 13,90 | 14,00 | 14,50 | - | ≈130 | 138,07 | 137,24 | 142,20 | - |
| i-$C_4H_{10}$ → 2-$C_3H_7$· + $CH_3$· | 16 | 16,30 | - | 17,70 | - | 325 | 343,09 | - | 352,31 | - |
| 1-$C_5H_{11}$· → $C_3H_7$· + $C_2H_4$ | 13,491 | 13,50 | 13,50 | 14,00 | - | 121 | 131,80 | 131,80 | 125,50 | - |
| 1-$C_5H_{11}$· → 2-$C_5H_{11}$· | 10,283 | - | 11,00 | 11,30 | - | 64,07 | - | 83,68 | 76,60 | - |
| 2-$C_5H_{11}$· → 1-$C_5H_{11}$· | 10,113 | - | 11,10 | 11,50 | - | 75,24 | - | 97,91 | 90,40 | - |
| 2-$C_5H_{11}$· → $C_3H_6$ + $C_2H_5$· | 13,7 | 12,60 | 12,60 | 14,00 | - | 123 | 120,08 | 120,08 | 129,70 | - |
| n-$C_5H_{12}$ → 1-$C_4H_9$· + $CH_3$· | 16,5 | - | 16,80 | 17,80 | - | 331,0 | - | 357,31 | 357,70 | - |
| n-$C_5H_{12}$ → 1-$C_3H_7$· + $C_2H_5$· | - | - | 16,80 | 17,10 | - | - | - | 342,67 | 341,40 | - |
| i-$C_5H_{12}$ →2-$C_4H_9$· + $CH_3$· | - | - | 17,10 | 17,50 | - | - | - | 346,85 | 351,50 | - |
| i-$C_5H_{12}$ → 2-$C_3H_7$· + $C_2H_5$· | - | - | 16,60 | 16,90 | - | - | - | 331,37 | 335,20 | - |
| i-$C_5H_{12}$ → i-$C_4H_9$· + $CH_3$· | - | - | 16,70 | 17,40 | - | - | - | 355,64 | 357,30 | - |
| 1-$C_6H_{13}$· → 2-$C_6H_{13}$· | 8-10 | - | 9,20 | 10,60 | - | 45-48 | - | 46,44 | 51,00 | - |
| 2-$C_6H_{13}$· → 1-$C_6H_{13}$· | 10,4 | - | 9,30 | 10,70 | - | 88,1 | - | 62,34 | 64,90 | - |
| i-$C_6H_{13}$· → 2-$C_3H_7$· + $C_3H_6$ | - | - | 13,40 | 14,00 | - | - | - | 117,99 | 121,30 | - |
| n-$C_6H_{14}$ → 1-$C_3H_7$· + 1-$C_3H_7$· | - | - | 16,50 | 16,50 | - | - | - | 342,67 | 342,70 | - |
| n-$C_6H_{14}$ → 1-$C_4H_9$· + $C_2H_5$· | - | - | 16,80 | 16,80 | - | - | - | 342,67 | 342,70 | - |
| i-$C_6H_{14}$ → 1-$C_3H_7$· + 2-$C_3H_7$· | - | - | 16,60 | 16,60 | - | - | - | 331,37 | 331,40 | - |
| i-$C_6H_{14}$ → i-$C_4H_9$· + $CH_3$· | - | - | 16,80 | 16,80 | - | - | - | 338,90 | 338,90 | - |
| i-$C_6H_{14}$ → 2-$C_5H_{11}$· + $CH_3$· | - | - | 17,10 | 17,10 | - | - | - | 346,85 | 346,90 | - |
| n-$C_7H_{16}$ → 1-$C_5H_{11}$· + $C_2H_5$· | - | - | 16,80 | 16,60 | - | - | - | 342,67 | 220,00 | - |
| n-$C_7H_{16}$ → 1-$C_6H_{13}$· + $CH_3$· | - | - | 16,80 | 16,30 | - | - | - | 357,31 | 300,00 | - |
| i-$C_7H_{16}$ → 2-$C_6H_{13}$· + $CH_3$· | - | - | 17,10 | 16,60 | - | - | - | 346,85 | 300,00 | - |
| $CH_3$· + $CH_3$· → $C_2H_6$ | ≈13 | - | 10,10 | 13,30 | 13,46 | - | - | 0,00 | 0,00 | 0,42 |
| $C_2H_3$· + $C_2H_3$· → $C_4H_6$ | 13 | - | 10,10 | 13,10 | 12,97 | - | - | 0,00 | 41,84 | 0,00 |
| $C_2H_4$ + H· → $C_2H_5$· | 11-13 | 13,00 | 13,00 | 14,00 | 14,33 | 3-6 | 6,28 | 6,28 | 8,40 | 18,41 |
| $C_2H_4$ + $CH_3$· → $C_2H_3$· + $CH_4$ | 12 | 13,00 | 13,00 | 12,80 | - | ≈60 | 54,39 | 54,39 | 62,70 | - |
| $C_2H_5$· + $CH_3$· → $C_3H_8$ | 13 | 12,50 | 12,50 | 13,00 | 13,27 | 0 | 0,00 | 0,00 | 0,00 | 0,00 |
| $C_2H_5$· + $C_2H_4$ → $C_2H_6$ + $CH_3$· | - | 12,50 | 12,50 | 12,50 | - | - | 79,50 | 79,50 | 79,50 | - |
| $C_2H_5$· + $C_2H_5$· → $C_4H_{10}$ | 13 | 11,60 | 11,60 | 12,30 | 12,81 | 0,0 | 0,00 | 0,00 | 0,00 | 0,00 |
| $C_2H_6$ + H· → $C_2H_5$· + $H_2$ | 13-14 | 14,00 | 14,00 | 13,90 | 14,85 | ≈40 | 40,58 | 40,58 | 33,40 | 54,39 |
| $C_2H_6$ + $CH_3$· → $C_2H_5$· + $CH_4$ | 13 | 14,60 | 14,60 | 13,00 | 13,72 | 75 | 69,04 | 69,04 | 49,80 | 74,48 |
| $C_3H_5$· + $CH_3$· → 1-$C_4H_8$ | 12,4 | 12,50 | 12,50 | 12,90 | 13,43 | 0 | 0,00 | 0,00 | 0,00 | 0,00 |
| $C_3H_6$ + H· → 1-$C_3H_7$· | 12-13 | 13,00 | 13,00 | 13,60 | 13,81 | ≈12.5 | 12,13 | 12,13 | 8,40 | 22,59 |
| $C_3H_6$ + H· → 2-$C_3H_7$· | 13 | 13,00 | 13,00 | 13,60 | 14,05 | ≈5 | 6,28 | 6,28 | 8,40 | 16,32 |
| $C_3H_6$ + $C_2H_5$· → $C_2H_6$ + $C_3H_5$· | 10,7 | 11,00 | 11,00 | 12,60 | 12,31 | 21,7 | 38,49 | 38,49 | 58,60 | 60,67 |
| 1-$C_4H_8$ + H· → 1-$C_4H_9$· | 12,2 | 13,00 | 13,00 | 13,90 | 13,73 | 7,83 | 5,02 | 5,02 | 8,40 | 21,76 |
| 2-$C_4H_8$ + H· → 2-$C_4H_9$· | 13 | 12,80 | - | 14,00 | 13,16 | ≈8.7 | 5,02 | - | 10,50 | 18,83 |
| i-$C_4H_8$ + H· → i-$C_4H_9$· | 12,5 | 14,00 | - | 14,00 | - | 11 | 5,02 | - | 8,40 | - |
| n-$C_4H_{10}$ + H· → 1-$C_4H_9$· + $H_2$ | 13 | 14,20 | 14,20 | 14,80 | 14,88 | ≈40 | 40,58 | 40,58 | 33,50 | 53,56 |
| n-$C_4H_{10}$ + H· → 2-$C_4H_9$· + $H_2$ | 14 | 14,00 | 14,00 | 14,80 | 14,72 | ≈35 | 35,15 | 35,15 | 33,50 | 42,26 |
| n-$C_4H_{10}$ + $CH_3$· → 1-$C_4H_9$· + $CH_4$ | 13 | 13,50 | 13,50 | 13,00 | 13,78 | 56,87 | 48,53 | 48,53 | 49,80 | 74,06 |

# Appendix C

# Typical data for naphtha cracking

The next two tables represent typical data for a naphtha cracking furnace, containing typical values for composition of the naphtha feed (Table C.1) and cracked gas composition (Table C.2).

These sets of data were used for modelling the furnace developed in this work.

Table C.1 - Typical naphtha composition.

| Component | Mass fraction |
|---|---|
| n-butane | 0.0663 |
| n-pentane | 0.1148 |
| i-pentane | 0.0977 |
| cyclopentane | 0.0067 |
| Methyl-cyclopentane | 0.0221 |
| n-hexane | 0.0913 |
| i-hexane | 0.1083 |
| cyclohexane | 0.0140 |
| n-heptane | 0.0531 |
| i-heptane | 0.0779 |
| Naphthenic – C7 | 0.0621 |
| n-octane | 0.0412 |
| i-octane | 0.0639 |
| Naphthenic – C8 | 0.0467 |
| n-nonane | 0.0192 |
| i-nonane | 0.0331 |
| Naphthenic – C9 | 0.0244 |
| n-decane | 0.0018 |
| i-decane | 0.0068 |
| Benzene | 0.0061 |
| Toluene | 0.0152 |
| Xylene | 0.0178 |
| Ethylbenzene | 0.0038 |
| Aromatic – C9 | 0.0052 |

Table C.2 - Typical cracked gas composition from naphtha cracking.

| Component | Mass fraction |
|---|---|
| Hydrogen | 0.0087 |
| Methane | 0.1436 |
| Acetylene | 0.0034 |
| Ethylene | 0.2762 |
| Ethane | 0.0352 |
| Methyl-acetylene / Propadiene | 0.0063 |
| Propylene | 0.1688 |
| Propane | 0.0048 |
| n-butane | 0.0135 |
| i-butane | 0.0004 |
| 1-butene | 0.0183 |
| 2-butene | 0.0103 |
| i-butene | 0.0291 |
| 1,3-butadiene | 0.0501 |
| Vinyl acetylene | 0.0004 |
| isoprene | 0.0064 |
| 2-methyl-2-butene | 0.0004 |
| 3-methyl-1-butene | 0.0010 |
| 3-methyl-1-butene | 0.0025 |
| n-pentane | 0.0110 |
| i-pentane | 0.0097 |
| cyclopentane | 0.0005 |
| 1-pentene | 0.0012 |
| 2-pentene | 0.0014 |
| Methyl-cyclopentane | 0.0010 |
| 1,3-pentadiene | 0.0069 |
| cyclopentadiene | 0.0158 |
| cyclopentene | 0.0033 |
| Methyl-cyclopentene | 0.0006 |

| Component | Mass fraction |
|---|---|
| n-hexane | 0.0048 |
| i-hexane | 0.0042 |
| cyclohexane | 0.0007 |
| cyclohexene | 0.0009 |
| 1,3-hexadiene | 0.0005 |
| 1-hexene | 0.0004 |
| C6 Olefins | 0.0006 |
| Methyl-cyclohexene | 0.0005 |
| n-heptane | 0.0015 |
| i-heptane | 0.0016 |
| 1-heptene | 0.0001 |
| C7 Olefins | 0.0002 |
| n-octane | 0.0006 |
| i-octane | 0.0008 |
| C8 Olefins | 0.0001 |
| n-nonane | 0.0002 |
| i-nonane | 0.0002 |
| Others | 0.0105 |
| Benzene | 0.0560 |
| Toluene | 0.0307 |
| Xylene | 0.0106 |
| Ethylbenzene | 0.0018 |
| Styrene | 0.0060 |
| Methyl-styrene | 0.0033 |
| di-methyl-styrene | 0.0007 |
| Other aromatics | 0.0003 |